DISASTER PREVENTION RESEARCH INSTITUTE
BULLETIN No. 63 JUNE, 1963

BASIC STUDIES ON THE CRITERION FOR SCOUR RESULTING FROM FLOWS DOWNSTREAM OF AN OUTLET

BY

YOSHITO TSUCHIYA

KYOTO UNIVERSITY, KYOTO, JAPAN

DISASTER PREVENTION RESEARCH INSTITUTE
KYOTO UNIVERSITY
BULLETIN

Bulletin No. 63 June, 1963

Basic Studies on the Criterion for Scour Resulting from Flows Downstream of an Outlet

By

Yoshito TSUCHIYA*

Contents

* Assistant Professor of Hydraulics, Disaster Prevention Research Institute, Kyoto University, Japan.

Basic Studies on the Criterion for Scour Resulting from Flows Downstream of an Outlet

Synopsis

As a first step to establish the mechanics of local scour, downstream of a culvert and an outlet, and to clarify the method for preventing local scour, the present paper deals with a theoretical consideration on the hydraulic behaviour of flows, downstream of an outlet, especially the boundary layer developing there, and a theory on the criterion for scour resulting from such flows, based on the results of detail experiments. Both theoretical results of the boundary layer development and the criterion for scour from flows, downstream of an outlet, are in good agreement with the results of experiments. Some contributions to design a procedure for the apron downstream of a culvert and an outlet are presented from the standpoint of the criterion for scour.

1. Introduction

In the past years, the design and planning of the apron at the downstream end of an outlet have usually been made by rule of thumb, to some extent, in determining the length of the apron required for maintenance of the outlet, as the mechanics of local scour resulting from flows has not been established yet because of complicated hydraulic phenomena.

Up to the present day no attempt has been made to derive a general conclusion on the local scour from the observations made on existing hydraulic works. According to Leliavsky[1], however, the methods for the design and planning of the apron may be divided into two different tendencies: the first one is to collect information on the hydraulic works which have either been built to the required dimensions from the start, or were subsequently strengthened until they were capable of permanently resisting the action of flow for local scour, and to derive a general conclusion from the analysis of such collected information, as the method of Bligh[2] proposed

in 1912; and the second, to perform the experiments or observations on the scour which occurs on the river bed downstream of the apron of existing hydraulic works, and to attempt to find general empirical laws applicable to practical purposes, as Leliavsky did, based on the suggestion by Khosla[3] The former method, the Bligh formula, was expressed by the relationship among the overfall width of the hydraulic works protecting the bed against scour, the discharge of flow, the height of the fall from the crest of a weir, or from the top of a shutter or a gate, down to the tail water level, and the coefficient characteristic of the material of a channel, on the basis of the observed results for the works preventing scour constructed in irrigation canals in India. It may be obvious of course that the hydraulic consideration of the Bligh formula should be questioned. However, the formula has been applied to practical problems in agricultural engineering because there are no hydraulic considerations on the protecting method against scour at the present time. The latter method was based on the measured results of scour holes in existing hydraulic works and their models. According to Khosla as an example, the depth of scour being a basic parameter in designing and planning hydraulic works is expressed by the term of total discharge for any given water level, on the basis of the fact that the length and width of the apron required for maintenance of the works are closely connected with the depth of scour.

On the other hand, the formula for the length of an apron derived by the U. S. War Department from the model tests at Iowa University in 1935 can be cited[3]. The formula is one of a few which aim at general applications as well as the Bligh formula described above. In the formula, the length of an apron is expressed by the relation including the discharge per unit width of the apron, the height of fall and the tail water depth, but no characteristics of bed materials. Besides, the studies concerned with the mechanism of local scour by Veronese[4] and Ahmad[5] can be cited. Since, however, the author's present study is to limited the criterion for scour from flows, the considerations on the mechanism of scour will not be given in detail.

Recently, Minami[6] studied the method for determining the length of an apron based on the characters of free turbulent jets after considering the Bligh formula. Since the results obtained on the critical tractive force were directly applied to estimate the length of the apron required for main-

tenance of the river bed, the study may be questioned, and a general formula for determining the length has not yet been obtained.

The hydraulic demand for design and planning of the length of an apron and its type is to reduce effectively the damage due to scour, or more strictly, to completely prevent the local scour. In this paper, based on the later demand the author investigates theoretically and experimentally basic relationships for determining the length of an apron under the condition that the sediment bed downstream of an apron is not absolutely scoured by action of flow.

In order to establish the mechanics of scour and a criterion for scour downstream of a culvert and an outlet, it is necessary, first of all, to analyze the characters of flows close to a bed, especially the boundary layer developing there. In the second chapter, therefore, the boundary layer growth in wall jets issuing from a submerged outlet is considered to be based on the momentum equation for a boundary layer connected with two-dimensional free turbulent jets. It is very difficult to analyze the boundary layer growth in wall jets having a free surface by solving the momentum equation. Therefore, the boundary layer growth in a free turbulent jet with a wall is analyzed, and the experiments of the resistance laws, the boundary layer growth and the diffusion of the wall jet are performed and compared with the theoretical results.

In the third chapter, the criterion for scour from wall jets issuing from a submerged outlet is considered theoretically, based on the procedure in the studies on the critical tractive force by the authors[7),8)]. by completely applying the characters of wall jets. The criterion for scour in the theory is defined as the criterion for movement of sands and gravels at or near the downstream end of an apron, and the apron to be considered is of a smooth bed. The theoretical results are compared with the experimental data by applying a new definition for movement of sands and gravels proposed by the author in the previous paper[9)] Furthermore, empirical formulas for the criterion and for determining the length of an apron necessary to prevent the river bed downstream of a submerged outlet from scour under the condition already described, are proposed, and design charts available to practical applications are presented. In addition, some considerations for the hydraulic design on the length of an apron are briefly described from the standpoint of the criterion for scour, and based on some examples for practi-

cal purposes.

2. Boundary Layer Growth in Wall Jets Issuing from a Submerged Outlet

The flows downstream of a culvert and an outlet are generally divided into two cases; the first is the case when the flow becomes a submerged jet or a submerged efflux, and the second, when the flow becomes super-critical flow. In the latter, the flow connects with the uniform flow downstream by hydraulic jump, and sometimes the flow runs on downstream in the state of super-critical flow. The boundary layer growth in this case had been studied by Halbronn[10], Craya and Delleur[11], Bauer[12] and in Japan, Iwasa[13], by applying the theory of a boundary layer. By using adequately, the results obtained by the above authorities, therefore, characters of the flow may be cleared. On the other hand, behaviors of the flow in the former case are complicated, and especially the general theoretical approach for solving such flows associated with jet diffusions may be very difficult. It may be the most important problem for disclosing the mechanism of local scour and the criterion for scour to analyze mathematically the flow characters in this case with the aid of experiments.

In the past years, as a study on the flow downstream of a culvert and an outlet, experimental investigations for determining the discharge coefficient of flow through the outlet were made. In 1950, Henry[14] investigated the same problems, and moreover, the internal mechanism of the flow, especially the exchange of hydraulic energy was considered. However, the boundary layer growth and characters of the flow were not cleared. Some experiments on the flow issuing from a submerged outlet were made by Tsubaki and Furuya[15] in 1952, and some characters of the flow, especially water surface profile, length of surface vortex and decrease in maximum velocity, were considered by comparing with the results of Henry and Albertson[16]

Recently, Glauert[17] investigated theoretically jet diffusion along a wall, which he named a wall jet. Subsequently Bakke[18] performed an experiment of a wall jet and compared it with Glauert's theoretical results. But it seems that, in his paper, there is a doubtful point in applying the resistance law to the basic equations. More recently, Schwarz and Cosart[19] investigated theoretically and experimentally the two-dimensional turbulent

wall jet after the author's investigation as is described in the following[20]. It was shown from the theoretical considerations that the nominal thickness of a boundary layer must vary as x which is the distance from an outlet and the maximum velocity must vary as the power of x. The values of the Reynolds shear stress, the Boussinesq exchange coefficient and the shear stress at the wall were evaluated from the detailed experimental results with the aid of a hot-wire anemometer.

In this chapter, with a different stand point from that by Glauert, the boundary layer growth in wall jets issuing from a submerged outlet is treated on the basis of the momentum equation for a boundary layer connected with two-dimensional turbulent jets, and furthermore, some experiments on the wall jets were performed. The theoretical results are compared with the experimental data and the limit of applicability of the theoretical results caused by existence of a free surface is briefly described.

(1) Theoretical consideration of the boundary layer growth in wall jets

With regard to the wall jet schematically shown in Fig. 1, application of the momentum relationships for one-dimensional flow to the main flow and the boundary layer of which the thickness δ is defined by the value of z satisfying $\partial\bar{u}/\partial z=0$ based on the assumption that the shearing stress is zero at $z=\delta$, leads the following equations ; for the main flow,

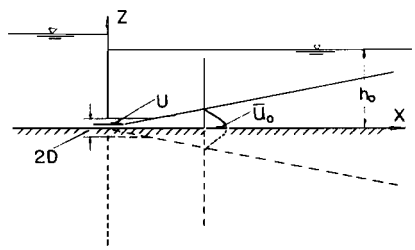

Fig. 1. Definition sketch of wall jet.

$$\frac{d}{dx}\int_{\delta}^{h}\{\rho\bar{u}^2+\rho\overline{u'^2}+p\}dz=0, \quad \cdots\cdots(1)$$

and for the boundary layer,

$$\frac{1}{u_0}\frac{d}{dx}\int_0^{\delta}\bar{u}dz-\frac{1}{u_0^2}\frac{d}{dx}\int_0^{\delta}\bar{u}^2dz=\frac{1}{\rho u_0^2}\int_0^{\delta}\frac{\partial p}{\partial x}dz+\frac{1}{u_0^2}\int\frac{\partial\overline{u'^2}}{\partial x}dz+\frac{C_f}{2}, \quad \cdots\cdots(2)$$

in which $\bar{u}$ is the time-average velocity component in the x-direction, u' the momentary departure from $\bar{u}$, u_0 the value of $\bar{u}$ at $z=\delta$, p the pressure, ρ the density of fluid, and C_f the local skin friction coefficient.

Now considering the case when $\delta=0$ and $h\to\infty$ in Eq. (1), and neglecting the pressure gradient resulting from velocity fluctuations, the case be-

comes suitable for a two-dimensional free jet. Some characters of the jet disclosed by early pioneers are described in the following, to consider theoretically the criterion for scour resulting from wall jets in the second chapter.

Researches on free turbulent jets were performed by many authorities, Tollmien[21], Kuethe[22] and Görtler[23], and also in 1950, Albertson and others[16] investigated theoretically the diffusion of jets based on the detailed experimentations. Tollmien and others studied the diffusion of jets, based on the fundamental equation,

$$\left.\begin{aligned} &\bar{u}\frac{\partial\bar{u}}{\partial x}+\bar{w}\frac{\partial\bar{u}}{\partial z}=\varepsilon_0\frac{\partial^2\bar{u}}{\partial z^2}, \\ &\partial\bar{u}/\partial x+\partial\bar{w}/\partial z=0, \end{aligned}\right\} \quad \cdots\cdots(3)$$

and by applying the assumption on the mixing length by Prandtl. In the above equation, $\bar{w}$ is the time-average velocity component in the z-direction, and ε_0 the eddy viscosity, which is constant by applying Prandtl's assumption taking the mixing length $l=cx$, in which c is a constant, and the fact that the center maximum velocity of a jet is proportional to $1/\sqrt{x}$. The solution of Eq. (3) by Görtler is written as

$$\left.\begin{aligned} &\frac{\bar{u}}{\bar{u}_0}=\operatorname{sech}^2\left(\sigma_0\frac{z}{x}\right), \\ &\frac{\bar{w}}{\bar{u}_0}=\frac{1}{2\sigma_0}\left\{2\sigma_0\frac{z}{x}\operatorname{sech}^2\left(\sigma_0\frac{z}{x}\right)-\tanh\left(\sigma_0\frac{z}{x}\right)\right\}, \end{aligned}\right\} \quad \cdots\cdots(4)$$

in which $\bar{u}_0$ is the center maximum velocity of a jet and σ_0 the constant expressed by $\sigma_0=(2\sqrt{2}c^2)^{-1/3}$.

On the other hand, according to the experimental results on the decrease in the center maximum velocity of a jet, the velocity $\bar{u}_0$ is constant from the outlet of a jet to a certain distance, where the jet remains potential flow and the region is known as a zone of flow establishment. At the far distance from the outlet the velocity is inversely proportional to the square root of a distance as described above, and the region is known as a zone of established flow. Then from the experimental results obtained by Albertson and others[16] the following relations can be written ; for the zone of flow establishment, $\xi\leq 2a^2$,

$$\bar{u}_0=U, \quad \cdots\cdots(5)$$

and for the zone of established flow, $\xi\geq 2a^2$,

$$\bar{u}_0/U=\sqrt{2}a/\sqrt{\xi}, \quad \cdots\cdots(6)$$

in which U is the velocity of a jet, $\xi = x/D$, D the opening of a jet, and α an empirical constant which is 2.28. Albertson and others investigated theoretically the velocity components of a jet by assuming that the velocity in the x-direction is expressed by the Gaussian curve,

$$\bar{u}/\bar{u}_0 = \exp(-z^2/\sigma^2), \quad \cdots\cdots(7)$$

in which σ is a variable proportional to x, and by applying the relation for the case when $\delta = 0$ and $h \to \infty$ in Eq. (1) and neglecting the static pressure and the pressure gradient resulting from velocity fluctuations.

It is very difficult to analyze the boundary layer growth in wall jets having a free surface by solving Eqs. (1) and (2) directly. Therefore, the boundary layer growth along the wall put in an apparent free turbulent jet with a wall, is treated, and the limit of applicability of the theoretical results is decided experimentally.

Considering $\partial p/\partial x = 0$ in a free turbulent jet and including the second term on the right in Eq. (2) into C_f, the momentum equation for the boundary layer is practically reduced to

$$\frac{1}{u_0}\frac{d}{dx}\int_0^\delta \bar{u}dz - \frac{1}{u_0^2}\frac{d}{dx}\int_0^\delta \bar{u}^2 dz = \frac{C_f}{2} \quad \cdots\cdots(8)$$

In Eq. (8), assuming that u_0 is approximately equal to $\bar{u}_0$, and using the suitable resistance law and the velocity profile, the boundary layer growth in wall jets can be discussed.

1) Laminar boundary layer growth

In the case of the laminar boundary layer, the velocity profile is assumed to be in the from of

$$\frac{\bar{u}}{u_0} = 2\left(\frac{x}{\delta}\right) - \left(\frac{z}{\delta}\right)^2 \quad \cdots\cdots(9)$$

Then, using the resistance law of laminar flow, and applying the relationship of u_0 in Eqs. (8) and (9) represented by Eqs. (5) and (6), the solution of Eq. (8) is obtained, with the boundary condition that $\delta = 0$ at $x = 0$, as follows:

for $\xi \leq 2\alpha^2$,

$$\zeta\left(\frac{UD}{\nu}\right)^{1/2} = \sqrt{30}\,\xi^{1/2}, \quad \cdots\cdots(10)$$

and for $\xi \geq 2\alpha^2$,

$$\zeta\left(\frac{UD}{\nu}\right)^{1/2} = \left(\frac{10\sqrt{2}}{3\alpha}\right)^{1/2}\xi^{-3/2}\{\xi^{9/2} + 56\sqrt{2}\alpha^9\}^{1/2}, \quad \cdots\cdots(11)$$

in which $\xi = x/D$, $\zeta = \delta/D$ and ν is the kinematic viscosity.

Then, the shear velocity u^* along the wall is expressed as follows: for $\xi \leq 2\alpha^2$,

$$\left(\frac{u^*}{U}\right)^2\left(\frac{UD}{\nu}\right)^{1/2} = \frac{2}{\sqrt{30}}\xi^{-1/2}, \quad \cdots\cdots(12)$$

and for $\xi \geq 2\alpha^2$,

$$\left(\frac{u^*}{U}\right)^2\left(\frac{UD}{\nu}\right)^{1/2} = 2\sqrt{2}\alpha\left(\frac{3\alpha}{10\sqrt{2}}\right)^{1/2}\xi\{\xi^{9/2}+56\sqrt{2\alpha^9}\}^{-1/2}. \quad \cdots\cdots(13)$$

2) Turbulent boundary layer growth

In the case of the turbulent boundary layer, the growth is analyzed, based on the power law; that is, the velocity profile is assumed to be

$$\bar{u}/u_0 = (z/\delta)^n, \quad \cdots\cdots(14)$$

in which $0 \leq n < 1$. Then, the relation between the local skin friction coefficient and the Reynolds number with respect to the nominal thickness of a boundary layer is written as

$$C_f = 2\lambda\left(\frac{u_0\delta}{\nu}\right)^{-2n/(n+1)}, \quad \cdots\cdots(15)$$

in which λ is a dimensionless empirical constant.

Applying the relationship of $\bar{u}_0$ described previously, to u_0 in Eqs. (8), (14) and (15), and denoting n and λ in Eqs. (14) and (15) by n and λ for $\xi \leq 2\alpha^2$, n_1 and λ_1 for $\xi \geq 2\alpha^2$ respectively, the following solutions of Eq. (8) are obtained: for $\xi \leq 2\alpha^2$, with the boundary condition that $\zeta = 0$ at $\xi = 0$,

$$\zeta\left(\frac{UD}{\nu}\right)^{2n/(3n+1)} = \left\{\frac{\lambda(2n+1)(3n+1)}{n}\right\}^{(n+1)/(3n+1)}\xi^{(n+1)/(3n+1)}, \quad \cdots\cdots(16)$$

and for $\xi \geq 2\alpha^2$, with the boundary condition that the value of ζ is equal to that in Eq. (16) at $\xi = 2\alpha^2$,

$$\zeta\left(\frac{UD}{\nu}\right)^{\frac{2n_1}{3n_1+1}} = (2)^{\frac{n_1+1}{3n_1+1}}(2\alpha^2)^{-\frac{n_1}{3n_1+1}} \times\left\{\frac{\lambda_1(2n_1+1)(3n_1+1)}{4n_1+1}\right\}^{\frac{n_1+1}{3n_1+1}}\xi^{-\frac{1}{2n_1}\{\xi^{\frac{4n_1+1}{2n_1}}+C\}^{\frac{n_1+1}{3n_1+1}}}, \quad \cdots(17)$$

in which

$$C = \frac{4n_1+1}{2\lambda_1(2n_1+1)(3n_1+1)}\left\{\frac{\lambda(2n+1)(3n+1)}{n}\right\}^{\frac{(n+1)(3n_1+1)}{(n_1+1)(3n+1)}}$$

$$\times(2\alpha^2)\left\{\frac{(n+1)(3n_1+1)}{(n_1+1)(3n+1)}+\frac{2n_1+1}{2n_1}\right\}\left(\frac{UD}{\nu}\right)\frac{2(n_1-n)}{(n+1)(n_1+1)}-(2\alpha^2)\frac{4n_1+1}{2n_1} \quad \cdots\cdots(18)$$

The shear velocity along the the wall is expressed as follows; for $\xi\leq 2\alpha^2$,

$$\left(\frac{u^*}{U}\right)^2\left(\frac{UD}{\nu}\right)^{2n/(3n+1)}=\lambda\left\{\frac{\lambda(2n+1)(3n+1)}{n}\right\}^{-2n/(3n+1)}\xi^{-2n/(3n+1)}, \quad \cdots\cdots(19)$$

and for $\xi\geq 2\alpha^2$,

$$\left(\frac{u^*}{U}\right)^2\left(\frac{UD}{\nu}\right)\frac{2n_1}{3n_1+1}=(2)^{-\frac{2n_1}{3n_1+1}}\lambda_1\left\{\frac{\lambda_1(2n_1+1)(3n_1+1)}{4n_1+1}\right\}^{-\frac{2n_1}{3n_1+1}}$$
$$\times(2\alpha^2)^{\frac{2n_1+1}{3n_1+1}}\left\{\xi^{\frac{2n_1+1}{2n_1}}+C\right\}^{-\frac{2n_1}{3n_1+1}} \quad \cdots\cdots(20)$$

In this case, when the shear velocity u^* is calculated by Eqs. (19) and (20), it becomes discontinuous at $\xi=2\alpha^2$ unless n and λ are equal to n_1 and λ_1 respectively. Since, however, the character of the flow, in fact, will change gradually in the vicinity of $\xi=2\alpha^2$, the discontinuity of u^* cannot occur.

It is concluded from the foregoing theoretical considerations that, for sufficiently large ξ, nominal thickness of boundary layer and the shear velocity are proportional to $\xi^{3/4}$ and $\xi^{-5/8}$ in the laminar boundary layer, and to $\xi^{(2n_1+1)/(3n_1+1)}$ and $\xi^{-2(3n_1+1)/(4n_1+1)}$ in the turbulent boundary layer respectively.

(2) Experiments on wall jets issuing from a submerged outlet

To verity the theoretical results, the boundary layer growth in wall jets issuing from outlets with openings of 0.56 cm and 1.08 cm was investigated. Velocity profiles were measured by the Pitot-tubes with outer-diameters of 0.070 cm and 0.200 cm, and the experiments were conducted with the suitable combinations of the Reynolds number at the outlet and the tail water depth.

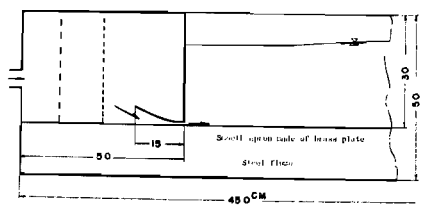

Fig. 2. Experimental apparatus.

1) Diffusion of wall jets

Fig. 3 represents some examples of the relationships between $\bar{u}_0/U$ and $x/2D$ in wall jets, and the solid line in the figure shows Albertson and others' result for a free turbulent jet. In this case, the method for estimation of the virtual maximum velocity of jet $\bar{u}_0$, is explained below.

As described above, since the velocity profiles of a free turbulent jet approximate to the Gaussian curve according to Albertson and others, the relationship between $\log \bar{u}$ and $(z/x)^2$ becomes straight. Therefore, the value of $\bar{u}_0$ is found by extending the straight line obtained by the data in the main flow to the line of $z/x=0$, and estimating $\bar{u}$ at $z/x=0$ from the intersection of these lines. It is seen from Fig. 3 that there exists a limit of applicability of the result for a free turbulent jet. From this reason, variations in the ratio of the limit x_c to h_0 with the Reynolds number at the outlet or the Froude number at the tail water is investigated as shown in Fig. 4, but the ratio x_c/h_0 is nearly constant for both parameters within the limit of the experiments.

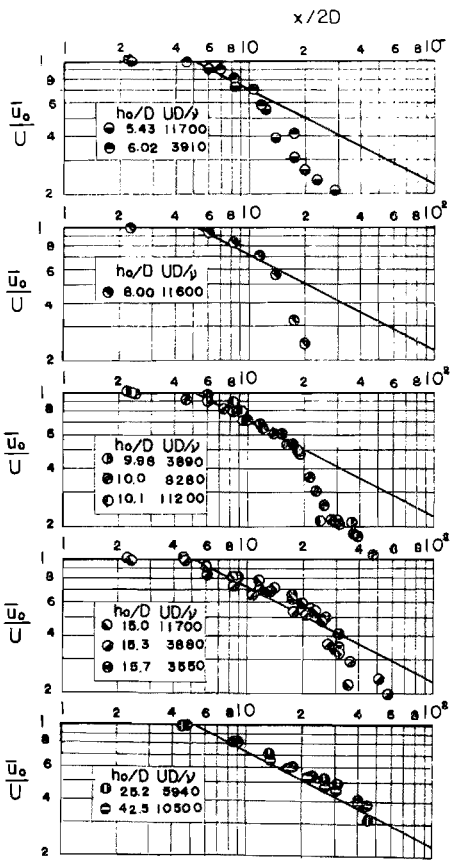

Fig. 3. Some examples of relationships between $\bar{u}_0/U$ and $x/2D$.

Fig. 5 shows some examples of comparisons between the measured velocity profiles in main flow and Görtler's and Gaussian curves. It is clear from the comparisons that the experimental results in the region of $\xi>2a^2$ are in good agreement with the theoretical curves of Görtler or Albertson and others for the range of $z/z_0<1$ except in the

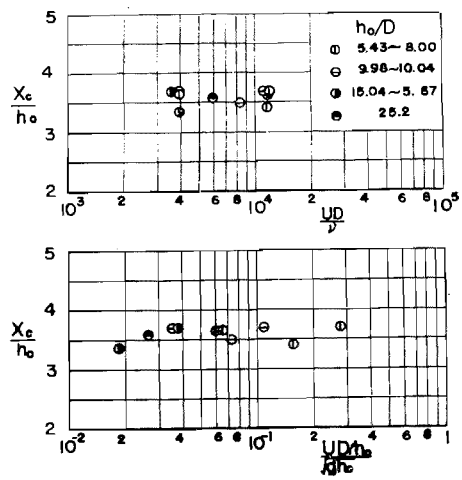

Fig. 4. Variation in x_c/h_0 with Reynolds number and Froude number.

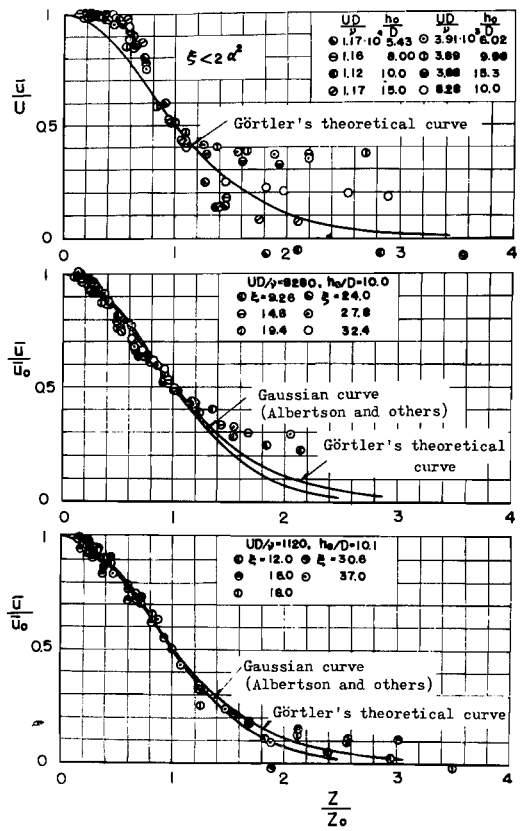

Fig. 5. Some examples of velocity profiles in main flow (z_0: the value of z corresponding to $\bar{u}=(1/2)\bar{u}_0$).

vicinity of a wall, where z_0 is the value of z corresponding to $\bar{u}=\bar{u}_0/2$, and contrarily are in disagreement with the curves in the region of $\xi<2a^2$.

Fig. 6 shows the variations in the width of a jet with a distance in the range of $\xi<\xi_c$, in which ξ_c is equal to x_c/D; and the same relation for a free turbulent jet is also presented in the figure for comparison. Besides, for the nominal width of jets, Tsubaki and Furuya, and Henry defined the nominal width as the minimum value of z, except $z=0$, satisfying $\bar{u}=0$, so their results are plotted higher than the author's. From the above experimental results, the mean value of the coefficient of mixing length, which is denoted by c, described already,

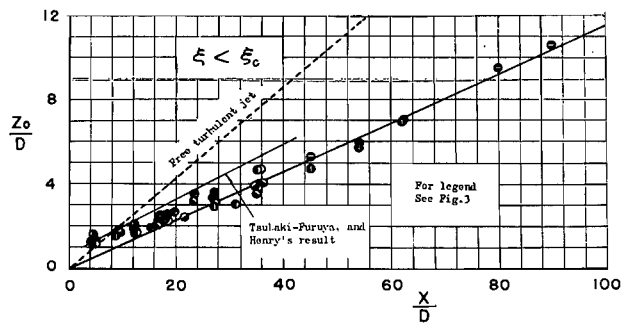

Fig. 6. Variations in width of wall jets in region of $\xi<\xi_c$ with distance.

has been estimated as $c=0.00858$.

2) Boundary layer growth

Fig. 7 represents some examples of velocity profiles in the boundary layer for the zone of established flow, $\xi>2\alpha^2$, and these results contain the experimental data for $UD/\nu=3380\sim11620$, $h_0/D=8.00\sim15.3$ and $\xi=11.9\sim35.0$. The solid line in the figure is for the case when $n=1/12$ in Eq. (14), while the plots of velocity profiles for $\xi<2\alpha^2$ show that the value of n is approximately equal to 1/7, that is the Blasius law. It has been confirmed from the semi-log plots of velocity profiles as is shown in Fig. 8 that

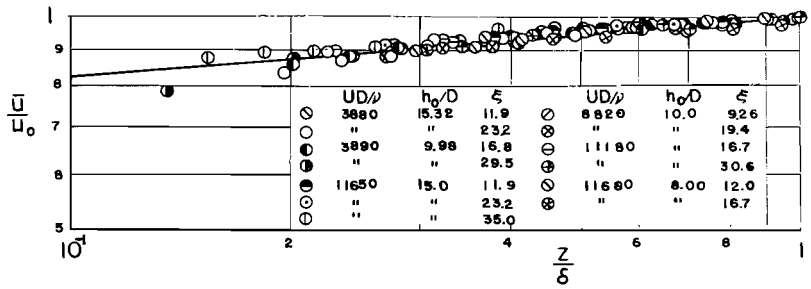

Fig. 7. Velocity profiles in boundary layer.

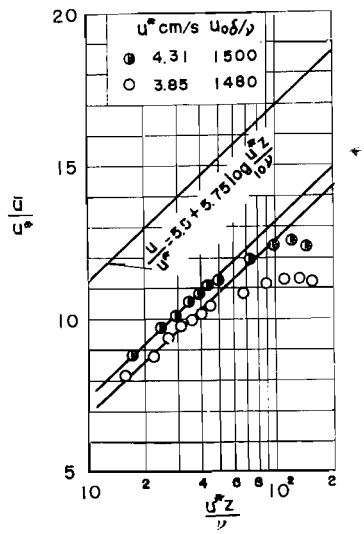

Fig. 8. Comparison between logarithmic law and experimental results of velocity profiles in boundary layer.

the logarithmic law is applicable in the vicinity of the bed.

Fig. 9 shows the variations in the local skin friction coefficient with the Reynolds number with respect to the nominal boundary layer thickness. Most of the data plotted in the figure were based on Eq. (8) from the measured velocity profiles and some data were estimated by applying the logarithmic law of velocity profile. For the latter, velocity profiles near the wall within about 1/10 of the nominal thickness should be measured[23], and therefore the Pitot-tube with an outer diameter of 0.070 cm was used. These results contain the data for $UD/\nu=2.4\times10^3\sim1.27\times10^4$ and $h_0/D=5.43\sim53.7$. It may be seen from the

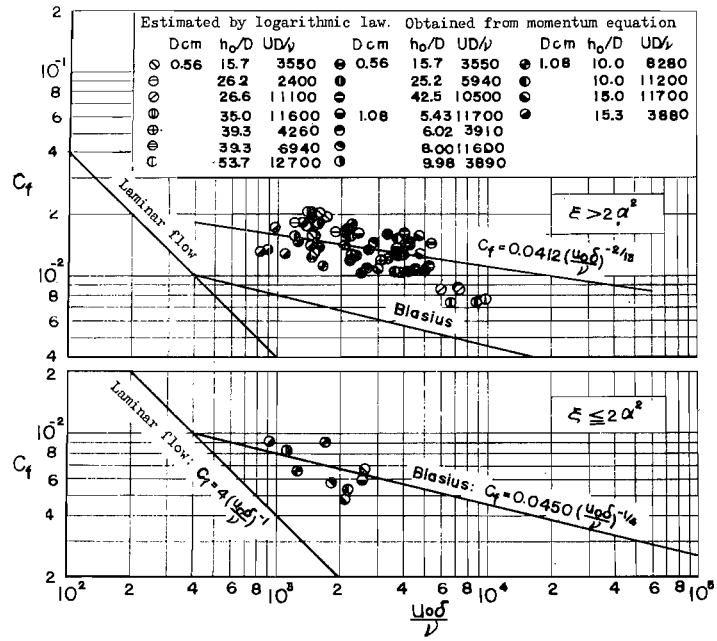

Fig. 9. Variations in local skin friction coefficient with Reynolds number of boundary layer.

figure that, although the Blasius law is applicable for $\xi<2\alpha^2$, the friction coefficient for $\xi>2\alpha^2$ is much greater than that by the Blasius law. It has been described by Schwarz and Cosart[19] that the mean value of the skin friction coefficient within the experiments is nearly equal to 0.01109 for the range of the Reynolds number of a boundary layer varying from 2.2×10^4 to 1.06×10^5, and at most, a slowly varying function of the Reynolds number of an outlet. As is seen in Fig. 9, the results agree well with the author's. It is evident that the character of jet diffusion in the region of $\xi<2\alpha^2$ is essentially different from that for $\xi>2\alpha^2$. However, the essential reason why the data for $\xi>2\alpha^2$ are considerably different from the Blasius law, cannot be explained because the effect of turbulence expressed by the second term on the right in Eq. (2) is not too little as to solve the question. And also no explanation can be given for that, in high Reynolds numbers, the values of C_f obtained by the momentum equation, are in disagreement with those estimated by the logarithmic law. It is, therefore, necessary for the interpretation of the essential reason, to measure directly the frictional stress

along the bed. However, for the time being, the resistance law presented by the data plotted is used for practical computation, and the boundary layer growth in wall jets is interpreted. Thus, the relation between C_f and $u_0\delta/\nu$ based on Eq. (15) is determined as the straight line shown in Fig. 9 by applying $n=1/12$.

Fig. 10 is an example of variations in the static pressure with the dis-

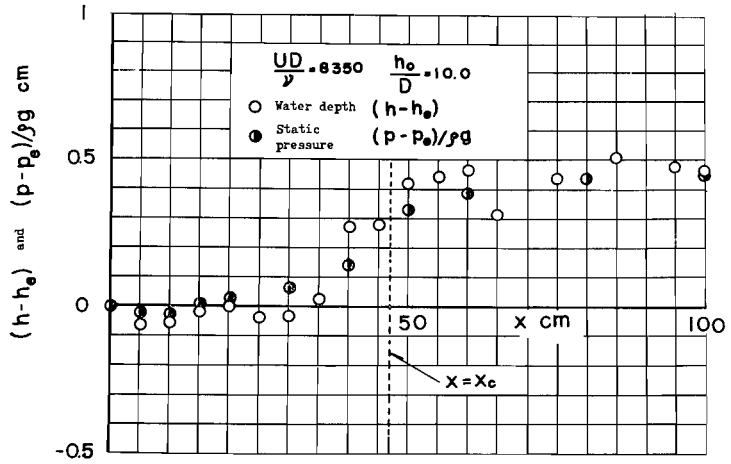

Fig. 10. Changes of static pressure and water depth with distance.

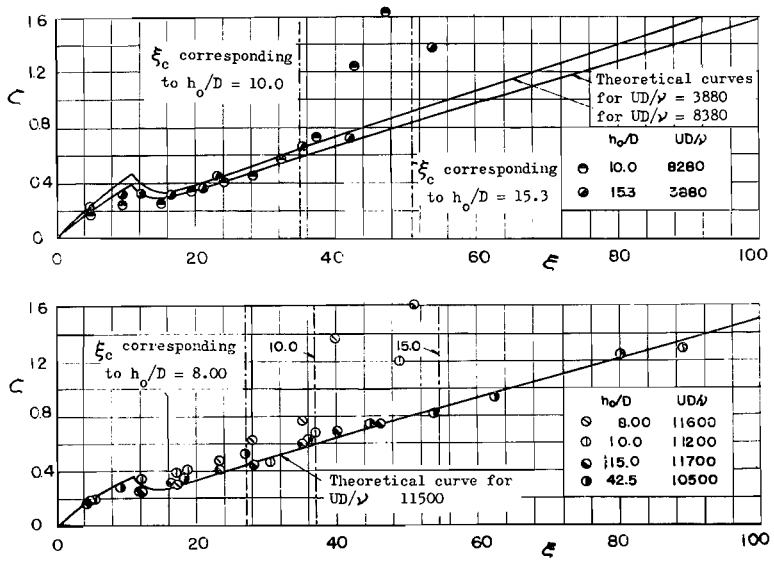

Fig. 11. Some examples of boundary layer growth.

tance from an outlet in a boundary layer. In the figure, h_e and p_e are respectively the water depth and the static pressure at the outlet. It is found from the results that the static pressure is nearly constant, that is $\partial p/\partial x \approx 0$, within a certain range close to the outlet, and the pressure gradient increases suddenly with the distance at or near $x = x_c$. The fact may indicate that the assumption that $\partial p/\partial x \approx 0$ in the boundary layer, in the theoretical consideration on the boundary layer growth, is approximately right.

Fig. 11 presents some examples of the experimental results and computations on the boundary layer growth. Since all experiments conducted by the author are for the turbulent boundary layer, as the resistance law, the Blasius law for $\xi \leq 2\alpha^2$ and the relation presented by the straight line in Fig. 9 for $\xi > 2\alpha^2$ have been applied in the computation of the boundary layer growth. The values of $\xi_c = x_c/D$ corresponding to h_0/D, obtained from Fig. 4, are shown in the figure. As is seen in the figure, the experimental data differ from the theoretical curves at these points. It may be concluded from the fact that x_c corresponds to the limit of applicability of the theoretical computation for the boundary layer growth.

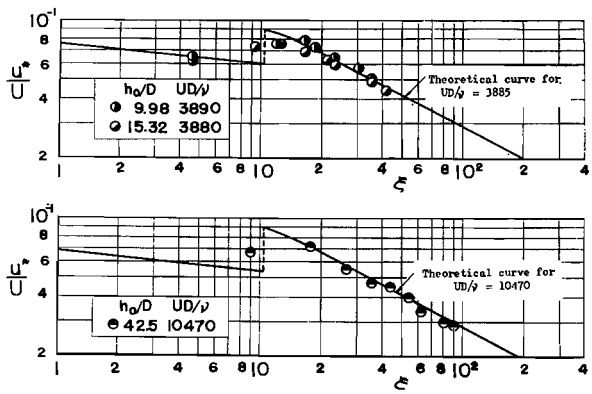

Fig. 12. Some examples of shear velocity distributions along bed.

Furthermore, Fig. 12 represents some examples of the shear velocity distributions along the bed for $\xi < \xi_c$ obtained by experiments and theoretical computations. The theoretical curves are in good agreement with the experimental results except for the data close to $\xi = 2\alpha^2$, where the resistance law changes gradually from the Blasius law to the other relation. It is concluded from the results that the shear velocity decreases rapidly with the

distance from the outlet, especially in the region of established flow, $\xi > 2a^2$. It is presumed by refering to Fig. 3 that the shear velocity will decrease extremely in the region of $\xi > \xi_c$ where the theoretical results on wall jets cannot be applied.

3. Criterion for Scour Resulting from Wall Jets Issuing from a Submerged Outlet

In this chapter, the criteria for scour resulting from wall jets issuing from a submerged outlet are considered theoretically by completely applying the results on wall jets obtained in the previous chapter. The definition of the criterion for scour in the theoretical consideration is the same as in the previous paper[9]; that is, sands and gravels at or near the downstream end of the apron downstream of an outlet are under the critical condition for the movement, and the apron to be considered is of a smooth bed.

In the theoretical approach to the criterion for scour, the theoretical development for the two regions described already, a zone of flow establishment and a zone of established flow, are obtained by applying the obtained results of wall jets and Spengos'[24] and Henry's[14] experimental results for characteristics of turbulence in the flows, and by the same procedure as in the theoretical consideration for the critical tractive force[7),8)] The theoretical considerations show that the criterion for scour resulting from wall jets can be expressed by the relation between $u_c{}^{*2}/(\sigma/\rho-1)gd \tan\varphi$ and $u_c{}^*d/\nu$ using the critical shear velocity $u_c{}^*$ in the same manner as for critical tractive forces, and furthermore, one parameter expressed by $u_c{}^*/u_0$ is added. This fact may be concerned with the development of a boundary layer, but it will be cleared from the comparisons between the theoretical curves and the experimental results for the criterion for scour that the parameter $u_c{}^*/u_0$ is not so important in the hydraulic mechanism as the other two parameters described already.

The experimental data have been obtained by applying the definition for the criterion for movement of sands and gravels proposed by the author in the preceeding paper[9], and compared with the theoretical curves for the criterion. Although some of the experimental data are quite scattered, the comparisons are fairly good.

In the third region in which the study of wall jets is not directly appli-

ed owing to the existence of a free water surface, the consideration for the criterion is made by means of dimensional analysis based on the characteristics of a wall jet, related to the criterion for scour in the first and second regions. It concluded from the consideration that for the criterion for scour in this region the ratio of the velocity of an outlet at the criterion for scour to the virtual velocity as a wall jet under the same condition can be presented closely by the parameter, the ratio of the tail water depth to the length of an apron.

In addition, empirical formulas for the criterion for scour in the three regions described above are proposed on the basis of both results of the theoretical considerations and the experimentations, and empirical formulas for determining the length of an apron under the criterion for scour are developed for practical uses. And moreover, some considerations on the design of the apron, especially in determining its length are described, and some practical examples are presented.

(1) Theoretical considerations on the criterion for scour resulting from wall jets

1) Equilibrium condition of a sand gravel

As is shown in Fig. 13, now consider the condition for criterion for movement of a sand gravel at or near the downstream end of an apron constructed downstream of an outlet by the same procedure as the hydrodynamical consideration for the critical tractive force by Iwagaki[7] By expressing the force relation shown in Fig. 14 as in Fig. 15, the equation for the equilibrium condition of a spherical sand gravel can be written as

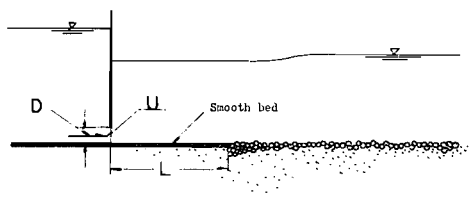

Fig. 13. Definition sketch of apron and flow downstream of submerged outlet.

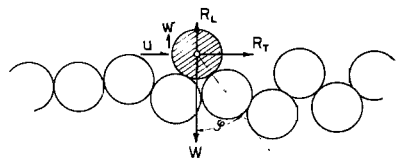

Fig. 14. Forces acting on a spherical sand gravel.

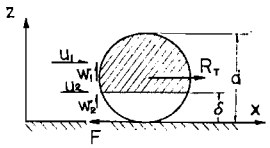

Fig. 15. Schematic diagram of force relation.

$$R_T=\{(\sigma-\rho)g(\pi/6)d^3-R_L\}\tan\varphi, \quad \cdots\cdots(21)$$

in which R_T is the sum of the fluid resistance and the resistance resulting from the pressure gradient in the direction of flow acting on a spherical sand gravel, R_L the uplift resulting from the pressure gradient in the vertical direction, σ and ρ the density of a spherical sand gravel and fluid respectively, d the diameter of a spherical sand gravel, g the acceleration of gravity, and φ the static friction angle of a spherical sand gravel.

Now let δ be the boundary layer thickness, and dividing the fluid resistance, denoted by R_T, acting on a spherical sand gravel, into two forces; the first is the resistance, denoted by R_{Tm}, acting on the gravel in the main flow and the second the resistance, denoted by R_{Tb}, acting on the gravel in the boundary layer, yields the following equation.

$$R_T=R_{Tm}+R_{Tb} \quad \cdots\cdots(22)$$

Let $\beta_s(\pi/4)d^2$ and $(1-\beta_s)(\pi/4)d^2$ be the cross sectional area of a spherical sand gravel exposed in a main flow in the direction of flow (shaded part in Fig. 15) and the area in a boundary layer, in which β_s is the function of δ/d only, the terms on the right in Eq. (22) are expressed respectively as

$$R_{Tm}=\frac{\rho}{2}C_{D1}u_1^2\beta_s\frac{\pi}{4}d^2-\left(\frac{\partial p}{\partial x}\right)_a d\beta_s\frac{\pi}{4}d^2, \quad \cdots\cdots(23)$$

$$R_{Tb}=\frac{\rho}{2}C_{D2}u_2^2(1-\beta_s)\frac{\pi}{4}d^2-\left(\frac{\partial p}{\partial x}\right)_\delta d(1-\beta_s)\frac{\pi}{4}d^2, \quad \cdots\cdots(24)$$

in which u_1 and u_2 are the representative velocities in the main flow and in the boundary layer respectively, C_{D1} and C_{D2} the drag coefficients corresponding to u_1 and u_2 respectively, and the second terms on the right in Eqs. (23) and (24) express the resistances resulting from the pressure gradient $\partial p/\partial x$ in the x-direction.

In the same manner as described above, the uplift R_L resulting from the pressure gradient in the z-direction is divided into R_{Lm} and R_{Lb} as follows:

$$R_L=R_{Lm}+R_{Lb} \quad \cdots\cdots(25)$$

and each term may be expressed as

$$R_{Lm}=\frac{\rho}{2}C_{Dw1}w_1^2A_1\frac{\pi}{4}d^2-\left(\frac{\partial p}{\partial z}\right)_a dA_1\frac{\pi}{4}d^2, \quad \cdots\cdots(26)$$

$$R_{Lb}=\frac{\rho}{2}C_{Dw2}w_2^2A_2\frac{\pi}{4}d^2-\left(\frac{\partial p}{\partial z}\right)_\delta dA_2\frac{\pi}{4}d^2, \quad \cdots\cdots(27)$$

in which, for $\delta\leq d/2$:

$$A_1=\left(1-\frac{\delta}{d}\right), \quad A_2=4\left(\frac{\delta}{d}\right)^2\left(1-\frac{\delta}{d}\right), \quad \cdots\cdots(28)$$

and for $\delta\geq d/2$:

$$A_1=4\left(\frac{\delta}{d}\right)\left(1-\frac{\delta}{d}\right)^2, \quad A_2=\frac{\delta}{d}. \quad \cdots\cdots(29)$$

and w_1 and w_2 are the representative velocities in the z-direction, in the main flow and in the boundary layer respectively, and C_{Dw1} and C_{Dw2} the drag coefficients corresponding to w_1 and w_2 respectively.

In order to evaluate the fluid resistances by the above equations, the theoretical analysis of both laminar and turbulent boundary layers and of the characteristics of turbulence in the boundary layers is necessary. However, the critical Reynolds number of a boundary layer in the transition from laminar to turbulent, the velocity profiles and the resistance laws close to the condition of the critical Reynolds number have not been made clear yet. Therefore, by assuming the fully developed laminar and turbulent boundary layers based on the power law, and estimating adequately the turbulence intencities in both, the main flow and boundary layer, the theoretical considerations on the criterion for scour are discussed in the following :

2) Theoretical consideration for the zone of flow establishment

As described already, the jet in the zone of flow establishment, $\xi\leq 2a^2$, is closely the potential flow having a constant velocity, and the nominal width of the jet decreases gradually straight to the point $\xi=2a^2$. The velocity profiles in this region are not sufficiently clarified.

In the theoretical consideration on the criterion for scour, therefore, the velocity profile is assumed to be uniform, and the scales of turbulence intencities in the flow are estimated, adequately based on some experimental results.

Under the above assumptions the second term on the right in Eq. (23) and all of Eq. (24) are abolished, but the effect of velocity fluctuations should be considered in estimating the fluid resistance resulting from time-average velocities.

(i) The case when the laminar boundary layer is assumed : It is as-

sumed that the velocity fluctuations do not exist in a laminar boundary layer. As velocity profiles in the boundary layer, Eq. (9) can be applied, and Eqs. (10) and (12) are used respectively for the boundary layer growth and for the distributions of shear velocities along a bed.

a) The case when $\delta \geq d$: In this case, the sand gravels are completely in the boundary layer, and then $R_{Tm}=0$, $\partial p/\partial x=0$ and $\beta_s=0$. Using the value of Eq. (9) at $z=d$ as the representative velocity, the fluid resistance R_T can be written as

$$R_T=\frac{\rho}{8}\pi d^2 u^{*2} C_{D2}\left(\frac{U}{u^*}\right)^2\left(\frac{d}{\delta}\right)^2\left\{2-\left(\frac{d}{\delta}\right)\right\}^2, \quad \cdots\cdots(30)$$

in which, from Eqs. (10) and (12) d/δ becomes

$$\frac{d}{\delta}=\frac{1}{2}\left(\frac{u^*}{U}\right)\left(\frac{u^* d}{\nu}\right). \quad \cdots\cdots(31)$$

The drag coefficient of a sphere C_{D2} in Eq. (30) can be expressed by the function of the Reynolds number as shown in Fig. 16. And the Reynolds number $u_2 d/\nu$ can be written as

$$R_{e2}=\frac{1}{2}\left(\frac{u^* d}{\nu}\right)^2\left\{2-\frac{1}{2}\left(\frac{u^*}{U}\right)\left(\frac{u^* d}{\nu}\right)\right\}. \quad \cdots\cdots(32)$$

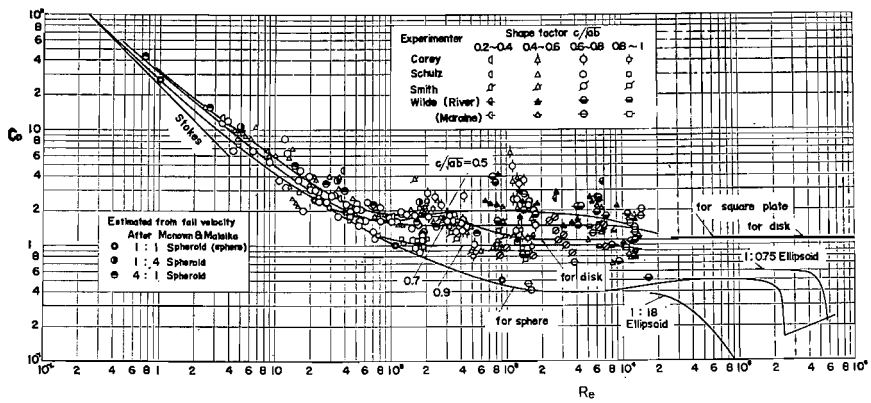

Fig. 16. Relation between drag coefficient of sphere and Reynolds number in comparison with other bodies'.

The velocity component $\overline{w}$ in the vertical, z-direction can easily be obtained by integrating the equation of continuity

$$\frac{\partial \overline{u}}{\partial x}+\frac{\partial \overline{w}}{\partial z}=0, \quad \cdots\cdots(33)$$

under the boundary condition that $\overline{w}=0$ at $z=0$. Calculating the value of $\overline{w}$ at $z=d$, denoted by w_2, from these results, taking into consideration that $\partial p/\partial z=0$ in the boundary layer and $\partial p/\partial x=0$ in this region, and inserting these results into Eq. (25) yields the following relation for the uplift

$$R_L=\frac{\rho}{8}\pi d^2 u^{*2} C_{Dw2}\left(\frac{15}{8}\right)^2\left(\frac{u^*}{U}\right)^6\left(\frac{u^*d}{\nu}\right)^4\left\{1-\frac{1}{3}\left(\frac{u^*}{U}\right)\left(\frac{u^*d}{\nu}\right)\right\}^2, \quad \cdots(34)$$

in which C_{Dw2} is the function of the Reynolds number expressed by

$$R_{ew2}=\frac{15}{8}\left(\frac{u^*}{U}\right)^3\left(\frac{u^*d}{\nu}\right)^3\left\{1-\frac{1}{3}\left(\frac{u^*}{U}\right)\left(\frac{u^*d}{\nu}\right)\right\}. \quad \cdots\cdots(35)$$

Inserting the above relationships into the equation of equilibrium condition expressed by Eq. (21) and rewriting the equation, the following relation can be obtained.

$$\frac{u_c^{*2}}{(\sigma/\rho-1)gd\tan\varphi}=\frac{4}{3\phi_1}. \quad \cdots\cdots(36)$$

in which

$$\phi_1=C_{D2}\left(\frac{u_c^*d}{\nu}\right)^2\left\{2-\frac{1}{2}\left(\frac{u_c^*}{U}\right)\left(\frac{u_c^*d}{\nu}\right)\right\}^2$$
$$+\left(\frac{15}{8}\right)^2 C_{Dw2}\left(\frac{u_c^*}{U}\right)^6\left(\frac{u_c^*d}{\nu}\right)^4\left\{1-\frac{1}{3}\left(\frac{u_c^*}{U}\right)\left(\frac{u_c^*d}{\nu}\right)\right\}^2\tan\varphi, \quad \cdots\cdots(37)$$

and it is evident that the limit of applicability of Eqs. (36) and (37) is $d/\delta\leq 1$.

b) The case when $\delta\leq d$: In this case, a part of the sand gravel is exposed beyond the boundary layer. The representative velocities u_1 and u_2 are equal to the velocity U in the main flow. In order to evaluate the fluid resistance acting on a spherical sand gravel, expressing the representative velocity as $u_1=(1+m)U$ under the assumption that the square mean values of velocity fluctuations are proportional to the time-average velocity based on the experimental results obtained by Henry[14] shown in Fig. 17,

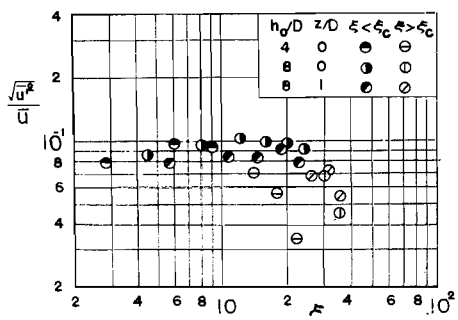

Fig. 17. Variations in turbulence intensity in wall jet issuing from submerged outlet with distance (after Henry, replotted by the author).

the fluid resistance R_T can be written as

$$R_T=\frac{\rho}{8}\pi d^2u^{*2}C_{D1}\left\{(1+m)^2\beta_s\left(\frac{U}{u^*}\right)^2+(1-\beta_s)\left(\frac{U}{u^*}\right)^2\right\}, \quad \cdots\cdots(38)$$

in which C_{D1} is the function of the Reynolds number expressed by

$$R_{e1}=\left(\frac{U}{u^*}\right)\left(\frac{u^*d}{\nu}\right). \quad \cdots\cdots(39)$$

The value of w_1 does not exist when calculated from the main flow, but the value exists, even though it is very small, when calculated from the boundary layer. Taking the calculated results in the latter, the uplift R_L can be expressed as

$$R_L=\frac{\rho}{8}\pi d^2u^{*2}C_{Dw2}\left(\frac{u^*}{U}\right)^2\left(\frac{5}{2}\right)^2A_2, \quad \cdots\cdots(40)$$

in which C_{Dw2} is the function of the Reynolds number expressed by

$$R_{ew2}=\frac{5}{2}\left(\frac{u^*}{U}\right)\left(\frac{u^*d}{\nu}\right). \quad \cdots\cdots(41)$$

Inserting these results into Eq. (21), the relationship corresponding to Eq. (36) can be obtained as follows.

$$\frac{u_c^{*2}}{(\sigma/\rho-1)gd\tan\varphi}=\frac{4}{3\phi_2}, \quad \cdots\cdots(42)$$

in which

$$\phi_2=C_{D1}\left(\frac{U}{u_c^*}\right)^2\{(1+m)^2\beta_s+(1-\beta_s)\}+\left(\frac{5}{2}\right)^2C_{Dw2}A_2\left(\frac{u_c^*}{U}\right)^2\tan\varphi. \cdots(43)$$

(ii) The case when the turbulent boundary layer is assumed: In the turbulent boundary layer in this region the Blasius 7th power law of velocity profile is established. The following theoretical consideration is developed for the general case.

Since it is necessary to consider the characters of turbulence in the turbulent boundary layer, the calculation for evaluating the characters of turbulence is made on the basis of the results of the hydrodynamical study on critical tractive forces by Iwagaki[7] and of the turbulence characters obtained by experimentations.

a) The case when $\delta\geq d$: As described above, in this case the sand gravels are completely in the boundary layer, and $\beta_s=0$. Now consider $\partial p/\partial x$ of the second term on the right in Eq. (23). The pressure gradient $\partial p/\partial x$ is generally the sum of that resulting from time-average ve-

locities and that resulting from fluctuating velocities. Since the velocity in the main flow U is constant in this case, the pressure gradient in the former vanishes, and also, that in the latter does not exist in the case of the laminar boundary layer. It is, however, necessary to consider the pressure gradient resulting from fluctuating velocities in the turbulent boundary layer.

In evaluating the pressure gradient $\partial p/\partial x$ resulting from fluctuating velocities, expressing $-\partial p/\partial x$ in Eq. (23) by $\rho Du/Dt$, based on the Eulerian equations of motion, and taking the statistical mean of the expression by the same procedure as Taylor[25] did by putting $u=\bar{u}+u'$ and $w=\overline{w}+w'$ in which $\bar{u}$ is the time-average velocity component in the x-direction, u' the momentary departure therefrom, that is the fluctuating velocity, $\overline{w}$ the time-average velocity component in the z-direction and w' the fluctuating velocity, the following relationship can be obtained:

$$-\frac{1}{\rho}\frac{\partial p}{\partial x}=\sqrt{\overline{u'^2}}\left\{\frac{\partial \bar{u}}{\partial x}+\sqrt{\overline{\left(\frac{\partial u'}{\partial x}\right)^2}}\right\}+\bar{u}\sqrt{\overline{\left(\frac{\partial u'}{\partial x}\right)^2}}$$
$$+\sqrt{\overline{w'^2}}\left\{\frac{\partial \bar{u}}{\partial z}+\sqrt{\overline{\left(\frac{\partial u'}{\partial z}\right)^2}}\right\}+\overline{w}\sqrt{\overline{\left(\frac{\partial u'}{\partial z}\right)^2}} \quad \cdots\cdots(44)$$

Introducing the scales of minimum eddies λ_{xx}, λ_{xz} and λ_{zx}, the pressure gradient becomes

$$-\frac{1}{\rho}\frac{\partial p}{\partial x}=\sqrt{\overline{u'^2}}\left\{\frac{\partial \bar{u}}{\partial x}+\sqrt{2}\frac{\sqrt{\overline{u'^2}}}{\lambda_{xx}}\right\}+\sqrt{2}\bar{u}\frac{\sqrt{\overline{u'^2}}}{\lambda_{xx}}$$
$$+\sqrt{\overline{w'^2}}\left\{\frac{\partial \bar{u}}{\partial z}+\sqrt{2\frac{\overline{u'^2}}{\lambda_{xx}^2}+\frac{1}{4\overline{u'^2}}\left(\frac{\partial \overline{u'^2}}{\partial z}\right)^2}\right\}+\overline{w}\sqrt{2\frac{\overline{u'^2}}{\lambda_{xx}^2}+\frac{1}{4\overline{u'^2}}\left(\frac{\partial \overline{u'^2}}{\partial z}\right)^2}$$
$$\cdots\cdots(45)$$

In order to calculate further the above equation, it must be clarified how the quantities $\bar{u}$, $\overline{w}$, $\overline{u'^2}$, $\overline{w'^2}$, λ_{xx}, λ_{xz} and λ_{zx} distribute vertically in the boundary layer.

Using the value expressed by Eq. (14) as time-average velocities in the x-direction $\bar{u}$, and calculating the time-average velocity component in the z-direction $\overline{w}$ from Eq. (33) by the same procedure as described already, the relation becomes

$$\overline{w}=U\left(\frac{z}{\delta}\right)^n\frac{d\delta}{dx} \quad \cdots\cdots(46)$$

Under the assumption that the values of the time-average velocity components $\bar{u}$ and $\overline{w}$ are used for representative velocities in calculating the

fluid resistances, the representative velocity u_2 takes the value of Eq. (4) at $z=d$, and inserting the result expressed by Eq. (16) into Eq. (46)

$$\frac{w_2}{U}=\frac{(n+1)(2n+1)}{n}(\lambda)^{-(n+1)/2}\left(\frac{u^*}{U}\right)^3\left(\frac{u^*d}{\nu}\right)^n \quad \cdots\cdots(47)$$

Now consider the fluctuating velocities expressed by square means in the boundary layer. Fig. 18 is the experimental results of distributions

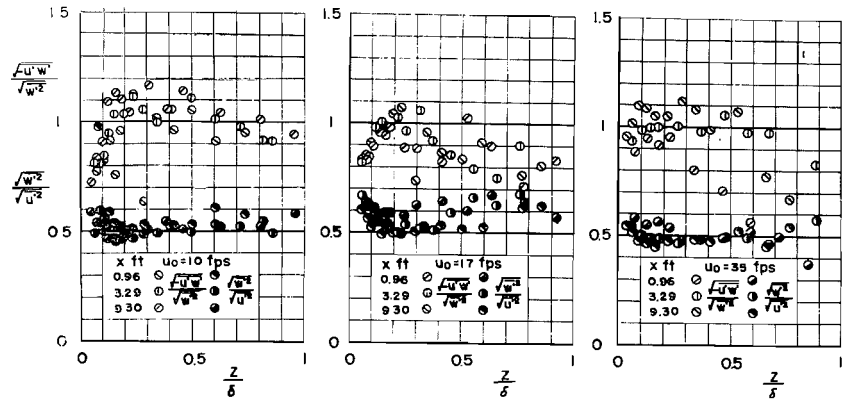

Fig. 18. Distributions of square means of fluctuating velocities in boundary layers with zero pressure gradient (after Spengos, replotted by the author).

of turbulence intensity, expressed by the ratios of turbulence intencities in each direction, in the boundary layers on a smooth flat plate in uniform flow obtained by Spengos[24] and replotted by the author. Although the experimental data are quite scattered it is found that the following relations assumed by Iwagaki[7] in the theoretical consideration on the critical tractive force can be applied in the boundary layer.

$$\sqrt{\overline{u'}^2}\approx 2u^*, \quad \sqrt{\overline{w'}^2}\approx u^* \quad \cdots\cdots(48)$$

The distributions of the scales of minimum eddies in boundary layers have not been clarified. Assuming that, therefore, the theory for isotropic turbulence can be applied to the relations among λ_{xx}, λ_{xz} and λ_{zz}, and that these scales are proportional to the mixing length l, the relations are written as

$$\lambda_{xx}=\sqrt{2}al, \quad \lambda_{xz}=\lambda_{zx}=al, \quad \cdots\cdots(49)$$

in which a is a constant which is not clear, but it will be about $a=12.5$ by estimating on the basis of Iwagaki's study on the critical tractive force.

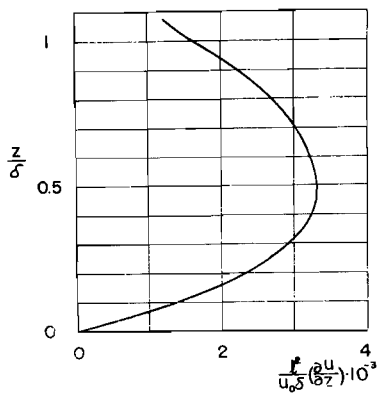

Fig. 19. Distribution of mixing length in boundary layer (after Spengos).

Furthermore, it is assumed that the experimental results, shown in Fig. 19, obtained by Spengos[24] in the boundary layer developing on a smooth flat plate can be applied in evaluating the distributions of the mixing length in the boundary layer developing in wall jets.

Evaluating the pressure gradient at $z=d$, denoted by $(\partial p/\partial x)_d$, by using the above relationships, and calculating the fluid resistance by applying the relation $u_2=\bar{u}+\sqrt{\overline{u'^2}}$ as Iwagaki did, the fluid resistance R_T can be written as

$$R_T=\frac{\rho}{8}\pi d^2u^{*2}C_{D2}\left\{(\lambda)^{-(n+1)/2}\left(\frac{u^*d}{\nu}\right)^n+2\right\}^2$$
$$+\frac{\rho}{4}\pi d^2u^{*2}\left[\frac{d}{al_d}\left\{2(2+\sqrt{2})+(\lambda)^{-(n+1)/2}\left(\frac{u^*d}{\nu}\right)^n\left(2+n\frac{al_d}{d}\right)\right\}\right.$$
$$-2(n+1)(2n+1)(\lambda)^{-(n+1)^2/2n}\left(\frac{u^*}{U}\right)^{(n+1)/n}\left(\frac{u^*d}{\nu}\right)^{n+1}$$
$$\left.+2\sqrt{2}\,\frac{(n+1)(2n+1)}{n}(\lambda)^{-(n+1)/2}\left(\frac{d}{al_d}\right)\left(\frac{u^*}{U}\right)^2\left(\frac{u^*d}{\nu}\right)^n\right], \quad \cdots\cdots(50)$$

in which l_d is the value of l at $z=d$ and C_{D2} the function of the Reynolds number expressed by

$$R_{\epsilon 2}=(\lambda)^{-(n+1)/2}\left(\frac{u^*d}{\nu}\right)^{n+1} \quad \cdots\cdots(51)$$

Now next consider the pressure gradient $\partial p/\partial z$ in the second term on the right in Eq. (27) by the same procedure as described above. Taking the statistical mean of $\partial p/\partial z$, it becomes

$$-\frac{1}{\rho}\frac{\partial p}{\partial z}=\sqrt{\overline{u'^2}}\left\{\frac{\partial \bar{w}}{\partial x}+\sqrt{\overline{\left(\frac{\partial w'}{\partial x}\right)^2}}\right\}+\bar{u}\sqrt{\overline{\left(\frac{\partial w'}{\partial x}\right)^2}}$$
$$+\sqrt{\overline{w'^2}}\left\{\frac{\partial \bar{w}}{\partial x}+\sqrt{\overline{\left(\frac{\partial w'}{\partial z}\right)^2}}\right\}+\bar{w}\sqrt{\overline{\left(\frac{\partial w'}{\partial z}\right)^2}} \quad \cdots\cdots(52)$$

Transforming the above equation as done in Eq. (45), Eq. (52) can be written as

$$-\frac{1}{\rho}\frac{\partial p}{\partial z}=\sqrt{\overline{u'^2}}\left\{\frac{\partial \overline{w}}{\partial x}+\sqrt{2}\frac{\sqrt{\overline{w'^2}}}{\lambda_{zx}}\right\}+\sqrt{2}\overline{u}\frac{\sqrt{\overline{w'^2}}}{\lambda_{zx}}$$
$$+\sqrt{\overline{w'^2}}\left\{\frac{\partial \overline{w}}{\partial z}+\sqrt{2}\frac{\sqrt{\overline{w'^2}}}{\lambda_{zz}}\right\}+\sqrt{2}\overline{w}\frac{\sqrt{\overline{w'^2}}}{\lambda_{zz}}. \quad \cdots\cdots(53)$$

Calculating the value of $(\partial p/\partial z)_a$ as done in evaluating R_T by applying the theoretical results for the isotropic turbulence to λ_{zz} in the above equation, and evaluating the fluid resistance by introducing the relation of $w_2=\overline{w}+\sqrt{\overline{w'^2}}$, the uplift R_L finally becomes

$$R_L=\frac{\rho}{8}\pi d^2u^{*2}C_{Dw2}\left\{\frac{(n+1)(2n+1)}{n}(\lambda)^{-(n+1)/2}\left(\frac{u^*}{U}\right)^2\left(\frac{u^*d}{\nu}\right)^n+1\right\}^2$$
$$+\frac{\rho}{4}\pi d^2u^{*2}\left[\frac{d}{al_a}\left[(1+2\sqrt{2})+(\lambda)^{-(n+1)/2}\left(\frac{u^*d}{\nu}\right)^n\left\{\sqrt{2}\right.\right.\right.$$
$$\left.\left.\left.+\frac{(n+1)(2n+1)}{n}\left(\frac{u^*}{U}\right)^2\right\}\right]+(n+1)(2n+1)(\lambda)^{-(n+1)/2}\right.$$
$$\times\left(\frac{u^*}{U}\right)^2\left(\frac{u^*d}{\nu}\right)^n\left\{1-\frac{(n+1)(2n+1)}{n}(\lambda)^{-(n+1)/2n}\left(\frac{u^*}{U}\right)^{(3n+1)/n}\left(\frac{u^*d}{\nu}\right)\right.$$
$$\left.\left.-\frac{4(2n+1)}{n}(\lambda)^{-(n+1)/2n}\left(\frac{u^*}{U}\right)^{(2n+1)/n}\left(\frac{u^*d}{\nu}\right)\right\}\right], \quad \cdots\cdots(54)$$

in which the drag coefficient C_{Dw2} is the function of the Reynolds number expressed by

$$R_{ew2}=\frac{(n+1)(2n+1)}{n}(\lambda)^{-(n+1)/2}\left(\frac{u^*}{U}\right)^2\left(\frac{u^*d}{\nu}\right)^{n+1} \quad \cdots\cdots(55)$$

Inserting the expressions for R_T and R_L into Eq. (21), the following relationship can finally be obtained.

$$\frac{u_c^{*2}}{(\sigma/\rho-1)gd\tan\varphi}=\frac{4}{3\phi_3}, \quad \cdots\cdots(56)$$

in which

$$\phi_3=C_{D2}\left\{(\lambda)^{-(n+1)/2}\left(\frac{u_c^*d}{\nu}\right)^n+2\right\}^2+2\left[\frac{d}{al_a}\left\{2(2+\sqrt{2})+(\lambda)^{-(n+1)/2}\right.\right.$$
$$\left.\times\left(\frac{u_c^*d}{\nu}\right)^n\left(2+n\frac{al_a}{d}\right)\right\}-2(n+1)(2n+1)(\lambda)^{-(n+1)^2/2n}\left(\frac{u_c^*}{U}\right)^{(2n+1)/n}$$
$$\left.\times\left(\frac{u_c^*d}{\nu}\right)^{n+1}+2\sqrt{2}\frac{(n+1)(2n+1)}{n}(\lambda)^{-(n+1)/2}\left(\frac{d}{al_a}\right)\left(\frac{u_c^*}{U}\right)^2\left(\frac{u_c^*d}{\nu}\right)^n\right]$$
$$+C_{Dw2}\left\{\frac{(n+1)(2n+1)}{n}(\lambda)^{-(n+1)/2}\left(\frac{u_c^*}{U}\right)^2\left(\frac{u_c^*d}{\nu}\right)^n+1\right\}^2\tan\varphi$$
$$+2\left[\frac{d}{al_a}\left\{(1+2\sqrt{2})+(\lambda)^{-(n+1)/2}\left(\frac{u_c^*d}{\nu}\right)^n\left\{\sqrt{2}\right.\right.\right.$$

$$+\frac{(n+1)(2n+1)}{n}\left(\frac{u_c^*}{U}\right)^2\Big\}\Big]+(n+1)(2n+1)(\lambda)^{-(n+1)/2}$$
$$\times\left(\frac{u_c^*}{U}\right)^2\left(\frac{u_c^* d}{\nu}\right)^n\Big\{1-\frac{(n+1)(2n+1)}{n}(\lambda)^{-(n+1)/2n}\left(\frac{u_c^*}{U}\right)^{(2n+1)/n}\left(\frac{u_c^* d}{\nu}\right)$$
$$-\frac{4(2n+1)}{n}(\lambda)^{-(n+1)/2n}\left(\frac{u_c^*}{U}\right)^{(2n+1)/n}\left(\frac{u_c^* d}{\nu}\right)\Big\}\Big]\tan\varphi, \quad \cdots\cdots(57)$$

and the condition of applicability is $(\lambda)^{-(n+1)/2n}(u_c^*/U)^{1/n}(u_c^* d/\nu)\leq 1$.

b) The case when $\delta\leq d$: In this case, a part of the sand gravel is exposed beyond the boundary layer. By the same procedure as in the laminar boundary layer the representative velocity is chosen and the effects of fluctuating velocities are evaluated. Applying the value at $z=\delta$ corresponding to the second term on the right in Eq. (50) for the resistance resulting from the pressure gradient in the boundary layer, the fluid resistance R_T can finally be written as

$$R_T=\frac{\rho}{8}\pi d^2 u^{*2} C_{D1}\Big\{(1+m)^2\beta_s\left(\frac{U}{u^*}\right)^2+(1-\beta_s)\left(\frac{U}{u^*}\right)^2\Big\}$$
$$+\frac{\rho}{4}\pi d^2 u^{*2}(1-\beta_s)\Big[\frac{d}{al_\delta}\Big\{2(2+\sqrt{2})+\left(\frac{U}{u^*}\right)\left(2+n\frac{al_\delta}{d}\right)$$
$$+2\sqrt{2}\,\frac{(n+1)(2n+1)}{n}\left(\frac{u^*}{U}\right)\Big\}-2(n+1)(2n+1)\left(\frac{u^*}{U}\right)\Big], \quad \cdots\cdots(58)$$

in which C_{D1} is the function of the Reynolds number expressed by Eq. (39) and l_δ the value of mixing length at $z=\delta$.

In the same manner, the uplift in the vertical direction R_L can finally be calculated as

$$R_L=\frac{\rho}{8}\pi d^2 u^{*2}\Lambda_2 C_{Dw2}\Big\{\frac{(n+1)(2n+1)}{n}\left(\frac{u^*}{U}\right)+1\Big\}^2+\frac{\rho}{4}\pi d^2 n^{*2}\Lambda_2$$
$$\times\Big[\frac{d}{al_\delta}\Big\{1+\sqrt{2}\left(2+\frac{U}{u^*}\right)+\frac{(n+1)(2n+1)}{n}\left(\frac{u^*}{U}\right)^2\Big\}$$
$$-\frac{2(n+1)(n+3)(2n+1)^2}{n}\left(\frac{u^*}{U}\right)^3+(n+1)(2n+1)\left(\frac{u^*}{U}\right)\Big], \quad \cdots\cdots(59)$$

in which C_{Dw2} is the function of the Reynolds number expressed by

$$R_{ew2}=\frac{(n+1)(2n+1)}{n}\left(\frac{u^*}{U}\right)\left(\frac{u^* d}{\nu}\right). \quad \cdots\cdots(60)$$

Inserting these results into the equation of equilibrium condition, the relation corresponding to Eq. (42) can be obtained as

$$\frac{u_c^{*2}}{(\sigma/\rho-1)gd\tan\varphi}=\frac{4}{3\phi_4}, \quad \cdots\cdots(61)$$

in which

$$\phi_4=C_{D1}\left(\frac{U}{u_c^*}\right)^2\{(1+m)^2\beta_s+(1-\beta_s)\}+2(1-\beta)\left[\frac{d}{al_\delta}\left\{2(2+\sqrt{2})\right.\right.$$
$$+\left(\frac{U}{u_c^*}\right)\left(2+n\frac{al_\delta}{\delta}\right)+2\sqrt{2}\,\frac{(n+1)(2n+1)}{n}\left(\frac{u_c^*}{U}\right)\Big\}$$
$$\left.-2(n+1)(2n+1)\left(\frac{u_c^*}{U}\right)\right]+A_2\left[C_{Dw2}\left\{\frac{(n+1)(2n+1)}{n}\left(\frac{u_c^*}{U}\right)+1\right\}^2\right.$$
$$+2\left(\frac{al_\delta}{d}\right)\left\{1+\sqrt{2}\left(2+\frac{U}{u_c^*}\right)+\frac{(n+1)(2n+1)}{n}\left(\frac{u_c^*}{U}\right)^2\right\}$$
$$\left.-\frac{2(n+1)(n+3)(2n+1)^2}{n}\left(\frac{u_c^*}{U}\right)^3+(n+1)(2n+1)\left(\frac{u_c^*}{U}\right)\right]\tan\varphi. \quad \cdots(62)$$

As described above, it is found that the criteria for scour in the region of the zone of flow establishment, $\xi\leq 2\alpha^2$, can be expressed by the following relationships for both cases of the laminar and the turbulent boundary layers.

$$\frac{u_c^{*2}}{(\sigma/\rho-1)gd\tan\varphi}=\frac{4}{3\phi_i}. \quad (i=1,\ 2,\ 3,\ 4) \quad \cdots\cdots\cdots\cdots(63)$$

in which

$$\phi_i=\phi_i\{u_c^*d/\nu,\ u_c^*/U\}. \quad \cdots\cdots\cdots\cdots(64)$$

Considering the relation $C_f=2(u_c^*/U)^2$ in calculating Eqs. (63) and (64), the values of u_c^*/U do not change much with the Reynolds number in practical cases. Therefore, Eq. (63) can be expressed by the relation between $u_c^{*2}/(\sigma/\rho-1)gd\tan\varphi$ and u_c^*d/ν with the parameter of u_c^*/U. Fig. 20 shows the relation between the friction coefficient C_f and the Reynolds number UL/ν based on the results shown in Fig. 9. When the criterion for scour is considered for the range of the Reynolds numbers of $UL/\nu=10^3\sim10^6$, it seems to be adequate to calculate Eqs. (63) and (64) for the ranges of u_c^*/U, from 0.1 to 0.06 for the laminar boundary layer

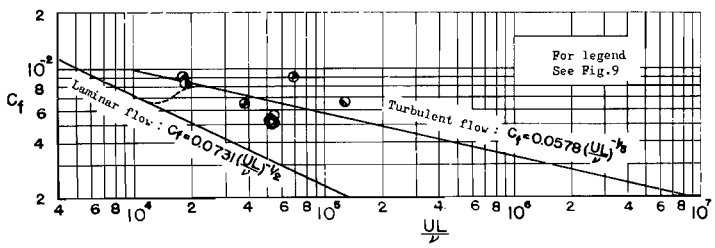

Fig. 20. Relation between C_f and UL/ν in region of $\xi\leq 2\alpha^2$.

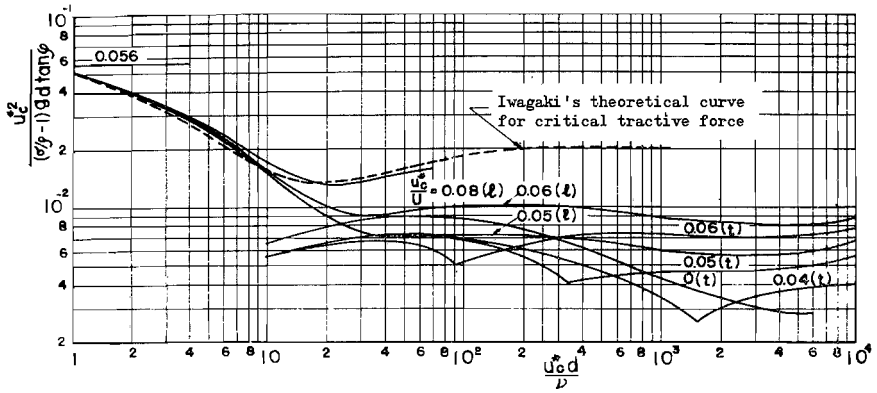

Fig. 21. Dimensionless expression of criterion for scour in zone of flow establishment obtained by the theory.

and from 0.06 to 0.04 for the turbulent boundary layer.

Fig. 21 presents the theoretical curves for the criterion for scour in this range calculated by using the assumption that $m=0.1$ based on the experimental results shown in Fig. 17. The notations of l and t show the theoretical curves in the laminar and the turbulent boundary layers respectively. The theoretical curve for the critical tractive force obtained by Iwagaki[7] is shown in the figure for comparison.

In addition, the value of $u_c{}^{*2}/(\sigma/\rho-1)gd\tan\varphi$ in Eq. (63) tends to approach 0.056 independently of the values of $u_c{}^*/U$ when the value of $u_c{}^*d/\nu$ becomes lesser than unity, and is equal to 0.056 in the range where the Stokes law can be applied to estimete the drag coefficient of a spherical sand gravel.

3) Theoretical consideration for the zone of established flow

In this region, the maximum velocity of a wall jet given by Eq. (6), and the boundary layer growth is expressed by Eq. (13) in the case of laminar boundary layers and by Eq. (17) in the case of turbulent boundary layers respectively.

It is difficult to consider the criterion for scour in this region by applying directly the results of the boundary layer growth obtained in the second chapter. The theoretical consideration for the criterion is made on the basis of the relationships neglecting the second terms in the brackets in Eqs. (11), (13), (17) and (19). This treatment is based upon the reasons why, as is seen in Fig. 13, the results of Eqs. (17) and (19) do not suf-

ficiently agree with the experimental data close to $\xi=2\alpha^2$ in the turbulent boundary layer and the effects of neglecting the second terms in the brackets in Eqs. (11), (13), (17) and (19), for the both laminar and turbulent boundary layers do not influence the ranges of slightly larger values of ξ than $2\alpha^2$. The theoretical results on the two-dimensional turbulent jet expressed by Eq. (4) are applied to the velocity profiles in a main flow, and moreover, Henry's experimental results already described are useful in evaluating the fluctuating velocities.

(i) The case when the laminar boundary layer is assumed : As just described in the preceding paragraph, it is assumed that the velocity fluctuations do not exist in the laminar boundary layer. The criterion for scour will be considered by dividing it into two cases ; one case is when the sand gravel is in the boundary layer and the other case is when a part of the sand ravel is exposed beyond the boundary layer.

a) The case when $\delta\geq d$: By using Eq. (19) for the velocity profile in the boundary layer and applying Eqs. (11) and (13) in which the second terms in the brackets on the right are neglected, the fluid resistance R_T can be written as follows by replacing U in Eqs. (30), (31) and (32) by u_0.

$$R_T=-\frac{\rho}{8}\pi d^2u^{*2}C_{D2}\left(\frac{u_0}{u^*}\right)^2\left(\frac{d}{\delta}\right)^2\left\{2-\left(\frac{d}{\delta}\right)\right\}^2, \quad \cdots\cdots(65)$$

in which

$$d/\delta=(1/2)(u^*/u_0)(u^*d/\nu)\cdots\cdots(66)$$

and the Reynolds number for C_{D2} can be written as

$$R_{e2}=\frac{1}{2}\left(\frac{u^*d}{\nu}\right)^2\left\{2-\frac{1}{2}\left(\frac{u^*}{u_0}\right)\left(\frac{u^*d}{\nu}\right)\right\}. \quad \cdots\cdots(67)$$

Taking into consideration that the velocity u_0 in Eq. (9) changes with the distance by the relation of Eq. (6), the velocity component w_2 in the z-direction at $z=d$ can be obtained from Eq. (33) as follows.

$$\frac{w_2}{u_0}=\frac{5}{12}\left(\frac{u^*}{u_0}\right)^4\left(\frac{u^*d}{\nu}\right)^2\left\{2-\frac{1}{2}\left(\frac{u^*}{u_0}\right)\left(\frac{u^*d}{\nu}\right)\right\}. \quad \cdots\cdots(68)$$

From the result, the uplift R_L can be written as

$$R_L=\frac{\rho}{8}\pi d^2u^{*2}C_{Dw2}\left(\frac{5}{12}\right)^2\left(\frac{u^*}{u_0}\right)^6\left(\frac{u^*d}{\nu}\right)^4\left\{2-\frac{1}{2}\left(\frac{u^*}{u_0}\right)\left(\frac{u^*d}{\nu}\right)\right\}^2, \quad \cdots(69)$$

in which C_{Dw2} is the function of the Reynolds number expressed by

$$R_{ew2}=\frac{5}{12}\left(\frac{u^*}{u_0}\right)^3\left(\frac{u^*d}{\nu}\right)^3\left\{2-\frac{1}{2}\left(\frac{u^*}{u_0}\right)\left(\frac{u^*d}{\nu}\right)\right\}. \quad \cdots\cdots(70)$$

Inserting above relationships into the equation of equilibrium condition, the following relation is finally reduced to

$$\frac{u_c{}^{*2}}{(\sigma/\rho-1)g\tan\varphi}=\frac{4}{3\phi_5}, \quad \cdots\cdots(71)$$

in which

$$\phi_5=\frac{1}{4}C_{D2}\left(\frac{u_c{}^*d}{\nu}\right)^2\left\{2-\frac{1}{2}\left(\frac{u_c{}^*}{u_0}\right)\left(\frac{u_c{}^*d}{\nu}\right)\right\}^2$$
$$+\left(\frac{5}{12}\right)^2C_{Dw2}\left(\frac{u_c{}^*}{u_0}\right)^6\left(\frac{u_c{}^*d}{\nu}\right)^4\left\{2-\frac{1}{2}\left(\frac{u_c{}^*}{u_0}\right)\left(\frac{u_c{}^*d}{u_0}\right)\right\}^2\tan\varphi \quad \cdots\cdots(72)$$

and it is obvious that the limit of applicability of this relation is $d/\delta\leq 1$.

b) The cases when $\delta\leq d$. Since a part of the sand gravel exposed beyond the boundary layer, the fluid resistance R_T is considered by dividing it into the two parts which are the fluid resistance in the boundary layer and that in the main flow. By the same treatment as in the consideration for the region of $\xi\leq 2a^2$ described already, the fluid resistance expressed by Eq. (14) can be written as

$$R_{Tb}=\frac{\rho}{8}\pi d^2u^{*2}C_{D2}(1-\beta_s)\left(\frac{u_0}{u^*}\right)^2, \quad \cdots\cdots(73)$$

in which C_{D2} is the function of the Reynolds number expressed by

$$R_{e2}=(u_0/u^*)(u^*d/\nu). \quad \cdots\cdots(74)$$

And by using the value at $z=\delta$ corresponding to Eq. (68) the uplift expressed by Eq. (27) can finally be written as

$$R_{Lb}=\frac{\rho}{8}\pi d^2u^{*2}C_{Dw2}\left(\frac{35}{18}\right)^2\Lambda_2\left(\frac{u^*}{u_0}\right)^2, \quad \cdots\cdots(75)$$

in which C_{Dw2} is the function of the Reynolds number expressed by

$$R_{ew2}=(35/18)(u^*/u_0)(u^*d/\nu), \quad \cdots\cdots(76)$$

and Λ_2 is represented by Eqs. (28) and (29) which is the function of d/δ expressed by Eq. (66).

Now next calculate the fluid resistance in the main flow. The relations of Eq. (14) using $c=0.00858$ which is the coefficient of mixing length in the wall jet as described already, can be applied to compute the velocity components of $\bar{u}$ and $\bar{w}$. Although the values of fluctuating velocities of $\sqrt{\bar{u}'^2}$ and $\sqrt{\bar{w}'^2}$ in the wall jet and the distributions have not been clarified yet,

the same relation that $\sqrt{\overline{u'^2}}=m\bar{u}$ as described already may also be applied to this region by considering that $\sqrt{\overline{u'^2}}/\bar{u}=$const. for the region of $\xi<\xi_c$ from the result shown in Fig. 17, and the same relation that $\sqrt{\overline{w'^2}}=m\bar{w}$ for the fluctuating velocity in the z-direction, as mentioned above, may be assumed.

Under the above treatments the first term on the right in Eq. (23) can be expressed by

$$R_{Tm1}=\frac{\rho}{8}\pi d^2u^{*2}C_{D1}(1+m)^2\beta_s\left(\frac{u_0}{u^*}\right)^2\mathrm{sech}^2\zeta_1, \quad \cdots\cdots(77)$$

in which C_{D1} is the function of the Reynolds number expressed by

$$R_{e1}=(u_0/u^*)(u^*d/\nu)\mathrm{sech}^2\zeta_1. \quad \cdots\cdots(78)$$

As is shown in Fig. 22, taking the value at $z=\delta$ for the representative velocity, the value of ζ_1 in Eq. (78) can be expressed as Eq. (79) by using Eq. (13) neglecting the second term in the bracket on the right side.

$$\zeta_1(=\sigma_0\delta/x)=(10/3)\sigma_0(u^*/u_0)^2 \quad \cdots\cdots(79)$$

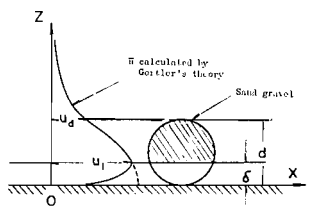

Fig. 22. Representative velocities in zone of established flow.

Since, as is seen in Fig. 5, the velocity of flow decreases rapidly with the distance from the bed, the fluid resistance may be evaluated too low if the value of velocity u_d at $z=d$ in the figure is taken for the representative velocity. On the other hand, as the velocity profiles in both cases of the critical tractive force and the criterion for scour at the downstream end of a smooth bed depend upon the logarithmic law, the fluid resistances have been evaluated higher than the true fluid resistances, and the theoretical results agree with the experimental data. Based on the above fact, therefore, the described treatment for the representative velocities has been assumed.

As described already, the first term on the right in Eq. (26) can be expressed by Eq. (80) with the aid of Eq. (4).

$$R_{Lm1}=\frac{\rho}{8}\pi d^2u^{*2}C_{Dw1}\left(\frac{1+m}{2\sigma_0}\right)^2\Lambda_1\left(\frac{u_0}{u^*}\right)^2(2\zeta_1\,\mathrm{sech}^2\zeta_1-\tanh\zeta_1)^2, \quad \cdots(80)$$

in which C_{Dw1} is the function of the Reynolds number expressed by

$$R_{ew1}=(1/2\sigma_0)(u_0/u^*)(u^*d/\nu)(2\zeta_1\,\mathrm{sech}^2\zeta_1-\tanh\zeta_1) \quad \cdots\cdots(81)$$

and Λ_1 is represented by Eqs. (28) and (29) which is the function of d/δ expressed by Eq. (66).

Next, consider the second term on the right in Eqs. (23) and (26). Although both of the pressure gradients of $\partial p/\partial x$ and $\partial p/\partial z$ are the sum of the pressure gradient resulting from time-average velocities and that resulting from fluctuating velocities as described already, the former of the two resistance may be considered to be negligible in the wall jet as applied in the analysis of boundary layer growth. In the region of $2a^2 \leq \xi < \xi_e$, therfore, only the pressure gradient resulting from the velocity fluctuations will be calculated in the same manner as described in the region of $\xi \leq 2a^2$.

Putting Eq. (4) and the fluctuating velocities expressed by the treatment described already into Eq. (35), expressing the scales of minimum eddies by the relations of Eq. (49), and considering that the mixing length in the wall jet is equal to $l=cx$, the second term on the right in Eq. (23) can be reduced to

$$R_{Tm2}=\frac{\rho}{4}\pi d^2 u^{*2}\beta_s\left(\frac{u_0}{u^*}\right)^2(\mathrm{sech}^4\zeta_1)\left[\frac{m(1+m)}{ac}\eta_1-m\eta_1\frac{\tanh\zeta_1}{\mathrm{sech}^2\zeta_1}\right.$$
$$\times(2\zeta_1\,\mathrm{sech}^2\zeta_1-\tanh\zeta_1)+m\eta_1\left(2\zeta_1\tanh\zeta_1-\frac{1}{2}\right)$$
$$\left.+\frac{m(1+m)}{\sigma_0}\eta_1\left(2\zeta_1-\frac{\tanh\zeta_1}{\mathrm{sech}^2\zeta_1}\right)\left\{\frac{1}{2(ac)^2}+\sigma_0^2\tanh\zeta_1\right\}^{1/2}\right], \quad \cdots\cdots(82)$$

in which

$$\eta_1(=d/x)=(5/3)(u^*/u_0)^3(u^*d/\nu), \quad \cdots\cdots(83)$$

and ζ_1 is expressed by Eq. (79).

By using Eq. (53) similarly, the second term on the right in Eq. (26) can finally be written as

$$R_{Lm2}=\frac{\rho}{4}\pi d^2 u^{*2}\Lambda_1\left(\frac{m}{2\sigma_0}\right)\left(\frac{u_0}{u^*}\right)^2(\mathrm{sech}^2\zeta_1)\left[2\zeta_1\eta_1(\mathrm{sech}^2\zeta_1)\right.$$
$$\times(2\zeta_1\tanh\zeta_1-1)+\tanh\zeta_1+2\sqrt{2}\left(\frac{m}{ac}\right)\eta_1(2\zeta_1\,\mathrm{sech}^2\zeta_1-\tanh\zeta_1)$$
$$+\left(2\zeta_1-\frac{\tanh\zeta_1}{\mathrm{sech}^2\zeta_1}\right)\left\{\frac{1}{2}\eta_1(1-4\zeta_1\tanh\zeta_1)\mathrm{sech}^2\zeta_1\right.$$
$$\left.\left.+\frac{(1+m)}{2ac\sigma_0}\eta_1(2\zeta_1\,\mathrm{sech}^2\zeta_1-\tanh\zeta_1)\right\}\right]. \quad \cdots\cdots(84)$$

Inserting these relationships into Eq. (21) and transforming the result, the criterion for scour in this region can be reduced to

$$\frac{u_c^{*2}}{(\sigma/\rho-1)gd\tan\varphi}=\frac{4}{3\phi_6}, \quad \cdots\cdots(85)$$

in which

$$\phi_6=\left(\frac{u_0}{u_c*}\right)^2\{(1+m)^2\beta_s C_{D1}\,\mathrm{sech}^4\zeta_1+(1-\beta_s)C_{D2}\}$$
$$+2\beta_s\left(\frac{u_0}{u_c*}\right)^2(\mathrm{sech}^4\zeta_1)\left[\frac{m(1+m)}{ac}\eta_1-m\eta_1\frac{\tanh\zeta_1}{\mathrm{sech}^2\zeta_1}(2\zeta_1\,\mathrm{sech}^2\zeta_1\right.$$
$$-\tanh\zeta_1)+m\eta_1\left(2\zeta_1\tanh\zeta_1-\frac{1}{2}\right)+\frac{m(1+m)}{\sigma_0}\eta_1\left(2\zeta_1-\frac{\tanh\zeta_1}{\mathrm{sech}^2\zeta_1}\right)$$
$$\times\left\{\frac{1}{2(ac)^2}+\sigma_0{}^2\tanh^2\zeta_1\right\}^{1/2}\Big]+2\left(\frac{u_c*}{u_0}\right)^2\left[\left(\frac{1+m}{2\sigma_0}\right)^2\Lambda_1 C_{Dw1}\right.$$
$$\times(2\zeta_1\,\mathrm{sech}^2\zeta_1-\tanh\zeta_1)^2+\left(\frac{35}{18}\right)^2\left.C_{Dw2}\Lambda_2\right]\tan\varphi$$
$$+\frac{m}{\sigma_0}\Lambda_1\left(\frac{u_0}{u_c*}\right)^2(\mathrm{sech}^2\zeta_1)\left[2\zeta_1\eta_1(\mathrm{sech}^2\zeta_1)(2\zeta_1\tanh\zeta_1-1)+\tanh\zeta_1\right.$$
$$+2\sqrt{2}\left(\frac{m}{ac}\right)\eta_1(2\zeta_1\,\mathrm{sech}^2\zeta_1-\tanh\zeta_1)+\left(2\zeta_1-\frac{\tanh\zeta_1}{\mathrm{sech}^2\zeta_1}\right)$$
$$\times\left\{\frac{1}{2}\eta_1(1-4\zeta_1\tanh\zeta_1)\,\mathrm{sech}^2\zeta_1\right.$$
$$\left.\left.+\frac{(1+m)}{2ac\sigma_0}\eta_1(2\zeta_1\,\mathrm{sech}^2\zeta_1-\tanh\zeta_1)\right\}\right]\tan\varphi. \quad\cdots\cdots(86)$$

(ii) The case when the turbulent boundary layer is assumed: In this region, the Blasius law for the resistance law in the turbulent boundary layer can not be applied, and the relationship shown in Fig. 9 should be used. But the theoretical consideration for the criterion is made for the general case as presented already. For the boundary layer growth and the distribution of shear velocity along the bed, Eqs. (11) and (19) neglecting the second term in brackets on the right are applied respectively.

a) The case when $\delta\geq d$: Using Eq. (14) replacing n by n_1 as velocity profiles, considering $\beta_s=0$ as formally done, and applying the relation expressed by Eq. (48) to evaluate the fluctuating velocities in the boundary layer as described already, the first term on the right in Eq. (23) can finally be reduced to

$$R_{Tb1}=\frac{\rho}{8}\pi d^2u^{*2}C_{D2}\left\{\left(\frac{u_0}{u^*}\right)\left(\frac{d}{\delta}\right)^{n_1}+2\right\}^2. \quad\cdots\cdots(87)$$

in which

$$d/\delta=(\lambda_1)^{-(n_1+1)/2n_1}(u^*/u_0)^{1/n_1}(u^*d/\nu), \quad\cdots\cdots(88)$$

and C_{D2} is the function of the Reynolds number expressed by

$$R_{e2}=(\lambda_1)^{-(n_1+1)/2n_1}(u^*/u_0)^{(1-n_1)/n_1}(u^*d/\nu)^2. \quad\cdots\cdots(89)$$

The uplift, which is expressed by the second term on the right in Eq. (23) resulting from the pressure gradient can be calculated by the same procedure as in the theoretical consideration for the zone of flow establishment. Applying Eq. (14) replacing n by n_1, and calculating the representative velocity w_2 corresponding to Eq. (47) from Eq. (43) the result can finally be reduced to

$$\frac{w_2}{u_0}=\left(\frac{d}{\delta}\right)^{n_1}\left\{\frac{(2n_1+1)(3n_1+1)}{(n_1+1)(4n_1+1)}(\lambda_1)^{-(n_1+1)/2n_1}\left(\frac{u^*}{u_0}\right)^{(2n_1+1)/n_1}\left(\frac{u^*d}{\nu}\right)\right.$$
$$\left.+\frac{2(n_1+1)(2n_1+1)}{4n_1+1}\left(\frac{u^*}{u_0}\right)^2\right\}. \quad \cdots\cdots(90)$$

Moreover, inserting Eqs. (14) and (90) into Eq. (45) under the assumption that the relations expressed by Eqs. (48) and (49) can be applied to the turbulance intensities of $\sqrt{\overline{u'^2}}$ and $\sqrt{\overline{w'^2}}$ and the scales of minimum eddies of λ_{xx}, λ_{xz} and λ_{zz}, respectively the second term on the right in Eq. (23) can be expressed as follows.

$$R_{Tb2}=\frac{\rho}{4}\pi d^2u^{*2}\left[\left(\frac{d}{al_d}\right)\left\{2(2+\sqrt{2})+(\lambda_1)^{-(n_1+1)/2}\left(\frac{u^*d}{\nu}\right)^{n_1}\right.\right.$$
$$\times\left(2+n_1\frac{al_d}{d}\right)\Big\}-\frac{4(2n_1+1)}{4n_1+1}(\lambda_1)^{-(n_1+1)/2}\left(\frac{u^*}{u_0}\right)^3\left(\frac{u^*d}{\nu}\right)^{n_1}$$
$$\times\left\{\frac{1}{2}(3n_1+1)(\lambda_1)^{-(3n_1+1)/2n_1}\left(\frac{u^*}{u_0}\right)^{1/n_1}\left(\frac{u^*d}{\nu}\right)+n_1(n_1+1)\right\}$$
$$+2\sqrt{2}\left(\frac{2n_1+1}{4n_1+1}\right)\left(\frac{d}{al_d}\right)(\lambda_1)^{-(n_1+1)/2}\left(\frac{u^*}{u_0}\right)^2\left(\frac{u^*d}{\nu}\right)^{n_1}$$
$$\left.\times\left\{\frac{3n_1+1}{n_1+1}(\lambda_1)^{-(n_1+1)/2n_1}\left(\frac{u^*}{u_0}\right)^{1/n_1}\left(\frac{u^*d}{\nu}\right)+2(n_1+1)\right\}\right]. \quad \cdots\cdots(91)$$

In the same manner as described above, calculating the relation corresponding to the first term on the right in Eq. (27) and also calculating the second term, the uplift corresponding to Eq. (54) can finally be written as

$$R_L=\frac{\rho}{8}\pi d^2u^{*2}C_{Dw2}\left(\frac{u_0}{u^*}\right)^2\left(\frac{d}{\delta}\right)^{2n_1}\left\{\frac{(2n_1+1)(3n_1+1)}{(n_1+1(4n_1+1)}(\lambda_1)^{-(n_1+1)/2n_1}\right.$$
$$\left.\times\left(\frac{u^*}{u_0}\right)^{(2n_1+1)/n_1}\left(\frac{u^*d}{\nu}\right)+\frac{2(n_1+1)(2n_1+1)}{4n_1+1}\left(\frac{u^*}{u_0}\right)^2\right\}^2$$
$$+\frac{\rho}{4}\pi d^2u^{*2}\left[2\left(\frac{u_0}{u^*}\right)\left(\frac{d}{\delta}\right)^{n_1}\left[n_1\left\{\frac{2(n_1+1)(2n_1+1)}{4n_1+1}\right\}^2\left(\frac{u^*}{u_0}\right)^2\left(\frac{d}{\delta}\right)\right.\right.$$
$$\left.\left.\times\left\{1+\frac{3n_1+1}{(n_1+1)^2}(\lambda_1)^{-(n_1+1)/2n_1}\left(\frac{u^*d}{\nu}\right)\left(\frac{u^*}{u_0}\right)^{1/n_1}\right\}\right.$$

$$+(3n_1+1)\left(\frac{2n_1+1}{4n_1+1}\right)^2(\lambda_1)^{-(3n_1+1)/n_1}\left(\frac{u^*d}{\nu}\right)^2\left\{\frac{3(3n_1+1)}{n_1+1}\right.$$
$$+2(n_1+1)\lambda_1\left(\frac{u^*d}{\nu}\right)^{-1}\left(\frac{u^*}{u_0}\right)^{1/n_1}+\frac{4n_1(n_1+1)}{3n_1+1}(\lambda_1)^{-(n_1+1)/2n_1}$$
$$\times\left(\frac{u^*d}{\nu}\right)^{-1}\left(\frac{u^*}{u_0}\right)^{(2n_1+1)/n_1}\Big\}+\frac{1}{\sqrt{2}}\left(\frac{d}{al_d}\right)+\frac{(2n_1+1)(3n_1+1)}{4n_1+1}$$
$$\times(\lambda_1)^{-(n_1+1)/2n_1}\left(\frac{u^*}{u_0}\right)^{(2n_1+1)/n_1}\left(\frac{u^*d}{\nu}\right)\Big]+(2\sqrt{2}+1)\left(\frac{d}{al_d}\right)\Big], \quad \cdots\cdots(92)$$

in which C_{D2} is the function of the Reynolds number expressed by

$$R_{ew2}=(\lambda_1)^{-(n_1+1)/2}\left(\frac{u^*d}{\nu}\right)^{n_1+1}\left\{\frac{(2n_1+1)(3n_1+1)}{(n_1+1)(4n_1+1)}(\lambda_1)^{-(n_1+1)/2n_1}\right.$$
$$\times\left(\frac{u^*}{u_0}\right)^{(2n_1+1)/n_1}\left(\frac{u^*d}{\nu}\right)+\frac{2(n_1+1)(2n_1+1)}{4n_1+1}\left(\frac{u^*}{u_0}\right)^2\Big\}, \quad \cdots\cdots(93)$$

and l_d shows the value of l obtaining from Fig. 19 by using the value of d/δ expressed by Eq. (88).

Inserting the fluid resistances of R_T and R_L obtained above into the equation of equilibrium condition, the criterion for scour in the range of $d/\delta\leq 1$ can be reduced to

$$\frac{u_c{}^{*2}}{(\sigma/\rho-1)gd\tan\varphi}=\frac{4}{3\phi_7}, \quad \cdots\cdots(94)$$

in which

$$\phi_7=C_{D2}\left\{\left(\frac{u_0}{u_c{}^*}\right)\left(\frac{d}{\delta}\right)^{n_1}+2\right\}^2+2\Big[\left(\frac{d}{al_d}\right)\Big\{2(2+\sqrt{2})+(\lambda_1)^{-(n_1+1)/2}$$
$$\times\left(\frac{u_c{}^*d}{\nu}\right)^{n_1}\left(2+n_1\frac{al_d}{d}\right)\Big\}-\frac{4(2n_1+1)}{4n_1+1}(\lambda_1)^{-(n_1+1)/2}\left(\frac{u_c{}^*}{u_0}\right)^3$$
$$\times\left(\frac{u_c{}^*d}{\nu}\right)^{n_1}\Big\{\frac{1}{2}(3n_1+1)(\lambda_1)^{-(3n_1+1)/2n_1}\left(\frac{u_c{}^*}{u_0}\right)^{1/n_1}\left(\frac{u_c{}^*d}{\nu}\right)$$
$$+n_1(n_1+1)\Big\}+2\sqrt{2}\left(\frac{2n_1+1}{4n_1+1}\right)\left(\frac{d}{al_d}\right)(\lambda_1)^{-(n_1+1)/2}\left(\frac{u_c{}^*}{u_0}\right)^2\left(\frac{u_c{}^*d}{\nu}\right)^{n_1}$$
$$\times\left\{\frac{3n_1+1}{n_1+1}(\lambda_1)^{-(n_1+1)/2n_1}\left(\frac{u_c{}^*}{u_0}\right)^{1/n_1}\left(\frac{u_c{}^*d}{\nu}\right)+2(n_1+1)\right\}\Big]+C_{Dw2}$$
$$\times\left(\frac{u_0}{u_c{}^*}\right)^2\left(\frac{d}{\delta}\right)^{2n_1}\left\{\frac{(2n_1+1)(3n_1+1)}{(n_1+1)(4n_1+1)}(\lambda_1)^{-(n_1+1)/2n_1}\left(\frac{u_c{}^*}{u_0}\right)^{(2n_1+1)/n_1}\right.$$
$$\times\left(\frac{u_c{}^*d}{\nu}\right)+\frac{2(n_1+1)(2n_1+1)}{4n_1+1}\left(\frac{u_c{}^*}{u_0}\right)^2\Big\}^2\tan\varphi+2\Big[2\left(\frac{u_0}{u_c{}^*}\right)\left(\frac{d}{\delta}\right)^{n_1}$$
$$\times\Big[n_1\Big\{\frac{2(n_1+1)(2n_1+1)}{4n_1+1}\Big\}^2\left(\frac{u_c{}^*}{u_0}\right)^2\left(\frac{d}{\delta}\right)\Big\{1+\frac{3n_1+1}{(n_1+1)^2}(\lambda_1)^{-(n_1+1)/2n_1}$$
$$\times\left(\frac{u_c{}^*d}{\nu}\right)\left(\frac{u_c{}^*}{u_0}\right)^{1/n_1}\Big\}+(3n_1+1)\Big\{\frac{2n_1+1}{4n_1+1}\Big\}^2(\lambda_1)^{-(3n_1+1)/n_1}$$

$$\times\left(\frac{u_c^*d}{\nu}\right)^2\left\{\frac{3(3n_1+1)}{n_1+1}+2(n_1+1)\lambda_1\left(\frac{u_c^*d}{\nu}\right)^{-1}\left(\frac{u_c^*}{u_0}\right)^{1/n_1}\right.$$
$$\left.+\frac{4n_1(n_1+1)}{3n_1+1}(\lambda_1)^{-(n_1+1)/2n_1}\left(\frac{u_c^*d}{\nu}\right)^{-1}\left(\frac{u_c^*}{u_0}\right)^{(2n_1-1)/n_1}\right\}$$
$$+\frac{1}{\sqrt{2}}\left(\frac{d}{al_a}\right)+\frac{(2n_1+1)(3n_1+1)}{4n_1+1}(\lambda_1)^{-(n_1+1)/2n_1}\left(\frac{u_c^*}{u_0}\right)^{(2n_1+1)/n_1}$$
$$\left.\times\left(\frac{u_c^*d}{\nu}\right)\right]+(2\sqrt{2}+1)\left(\frac{d}{al_a}\right)\Big]\tan\varphi. \quad \cdots\cdots(95)$$

b) The case when $\delta\leq d$: Since the sand grevels are exposed beyond the boundary layer in this case, both fluid resistances of R_{Tm} and R_{Tb} exist. Consider at first R_{Tb}. Calculating the relation corresponding to Eq. (91), the fluid resistance R_{Tb} can be obtained by the same procedure as in Eq. (58) as follows.

$$R_{Tb}=\frac{\rho}{8}\pi d^2u^{*2}C_{D2}(1-\beta_s)\left\{\left(\frac{u_0}{u^*}\right)+2\right\}^2+\frac{\rho}{4}\pi d^2u^{*2}(1-\beta_s)$$
$$\times\left[\left(\frac{d}{al_\delta}\right)\left\{2(2+\sqrt{2})+\left(2+n_1\frac{al_\delta}{\delta}\right)\left(\frac{u_0}{u^*}\right)\right\}\right.$$
$$-\frac{2(2n_1+1)(2n_1^2+5n_1+1)}{4n_1+1}\left(\frac{u^*}{u_0}\right)$$
$$\left.+2\sqrt{2}\,\frac{(2n_1+1)(2n_1^2+10n_1+3)}{(n_1+1)(4n_1+1)}\left(\frac{d}{al_\delta}\right)\left(\frac{u^*}{u_0}\right)\right], \quad \cdots\cdots(96)$$

in which C_{D2} is the function of the same Reynolds number as Eq. (74).

Since Eq. (4) can be applied to the velocity profile in the main flow, R_{Tm} becomes finally equal to the sum of Eqs. (77) and (82), and the following relations can be used for ζ_1 and η_1 in the equations.

$$\zeta_1\left(=\sigma_0\frac{\delta}{x}\right)=2\sigma_0\frac{(2n_1+1)(3n_1+1)}{4n_1+1}\left(\frac{u^*}{u_0}\right)^2, \quad \cdots\cdots(97)$$

and

$$\eta_1\left(=\frac{d}{x}\right)=2\lambda_1\frac{(2n_1+1)(3n_1+1)}{4n_1+1}(\lambda_1)^{-(3n_1+1)/2n_1}\left(\frac{u^*}{u_0}\right)^{(2n_1+1)/n_1}\left(\frac{u^*d}{\nu}\right). \quad \cdots\cdots(98)$$

By the same treatment as described above, R_{Lb} can be written as

$$R_{Lb}=\frac{\rho}{8}\pi d^2u^{*2}C_{Dw2}\Lambda_2\left\{\frac{(2n_1+1)(2n_1^2+10n_1+3)}{(n_1+1)(4n+1)}\left(\frac{u^*}{u_0}\right)+1\right\}^2$$
$$+\frac{\rho}{4}\pi d^2u^{*2}\Lambda_2\left[2\left(\frac{u_0}{u^*}\right)\left[\frac{4n_1(2n_1+1)^2(n_1^2+5n_1+2)}{(4n_1+1)^2}\left(\frac{u^*}{u_0}\right)^2\right.\right.$$
$$\left.\left.+\frac{(3n_1+1)(2n_1+1)^2}{(4n_1+1)^2}(\lambda_1)^{-2}\left(\frac{u^*}{u_0}\right)^4\left\{\frac{3(3n_1+1)}{n_1+1}\right.\right.\right.$$

$$+2(n_1+1)(\lambda)^{(n_1-1)/2n_1}\left(\frac{u^*}{u_0}\right)^{2/n_1}$$
$$+\frac{4n_1(n_1+1)}{(3n_1+1)}(\lambda_1)^{-(n_1+1)/n_1}\left(\frac{u^*}{u_0}\right)^2\Bigg\}+\frac{(2n_1+1)(3n_1+1)}{4n_1+1}\left(\frac{u^*}{u_0}\right)^2$$
$$+\frac{1}{\sqrt{2}}\left(\frac{d}{al_\delta}\right)\Bigg]+(1+2\sqrt{2})\left(\frac{d}{al_\delta}\right)\Bigg], \quad \cdots\cdots(99)$$

in which C_{Dw2} is the function of the Reynolds number expressed by

$$R_{ew2}=\frac{(2n_1+1)(2n_1^2+10n_1+3)}{(n_1+1)(4n_1+1)}\left(\frac{u^*}{u_0}\right)\left(\frac{u^*d}{\nu}\right). \quad \cdots\cdots(100)$$

For the uplift R_{Lm} in the main flow, the relations expressed by Eqs. (80) and (84) replacing ζ_1 and η_1 in these equations by Eqs. (97) and (98) respectively can be applied.

Inserting the results obtained above into the equation of equilibrium condition, the criterion for scour in the range of $d\geq\delta$ can finally be written as

$$\frac{u_c{}^{*2}}{(\sigma/\rho-1)gd\tan\varphi}=\frac{4}{3\phi_8}, \quad \cdots\cdots(101)$$

in which

$$\phi_8=(1+m)^2\beta_s\left(\frac{u_0}{u_c^*}\right)^2C_{D1}\,\mathrm{sech}^4\zeta_1+(1-\beta_s)C_{D2}\left\{\left(\frac{u_0}{u_c^*}\right)+2\right\}^2$$
$$+2(1-\beta_s)\left[\left(\frac{d}{al_\delta}\right)\left\{2(2+\sqrt{2})+\left(2+n_1\frac{al_\delta}{\delta}\right)\left(\frac{u_0}{u_c^*}\right)\right\}\right.$$
$$-\frac{2(2n_1+1)(2n_1^2+5n_1+1)}{4n_1+1}\left(\frac{u_c^*}{u_0}\right)+2\sqrt{2}\,\frac{(2n_1+1)(2n_1^2+10n_1+3)}{(n_1+1)(4n_1+1)}$$
$$\left.\times\left(\frac{d}{al_\delta}\right)\left(\frac{u_c^*}{u_0}\right)\right]+2\beta_s\left(\frac{u_0}{u_c^*}\right)^2(\mathrm{sech}^4\zeta_1)\left[\frac{m(1+m)}{ac}\eta_1\right.$$
$$-m\eta_1\frac{\tanh\zeta_1}{\mathrm{sech}^2\zeta_1}(2\zeta_1\,\mathrm{sech}^2\zeta_1-\tanh\zeta_1)+m\eta_1\left(2\zeta_1\tanh\zeta_1-\frac{1}{2}\right)$$
$$\left.+\frac{m(1+m)}{\sigma_0}\eta_1\left(2\zeta_1-\frac{\tanh\zeta_1}{\mathrm{sech}^2\zeta_1}\right)\left\{\frac{1}{2(ac)^2}+\sigma_0{}^2\tanh^2\zeta_1\right\}^{1/2}\right]$$
$$+2\left(\frac{u_c^*}{u_0}\right)^2A_1\left[\left(\frac{1+m}{2\sigma_0}\right)^2C_{Dw1}(2\zeta_1\,\mathrm{sech}^2\zeta_1-\tanh\zeta_1)^2\right.$$
$$+\frac{m}{2\sigma_0}(\mathrm{sech}^2\zeta_1)\left[2\zeta_1\eta_1(\mathrm{sech}^2\zeta_1)(2\zeta_1\tanh\zeta_1-1)+\tanh\zeta_1\right.$$
$$+2\sqrt{2}\left(\frac{m}{ac}\right)\eta_1(2\zeta_1\,\mathrm{sech}^2\zeta_1-\tanh\zeta_1)+\left(2\zeta_1-\frac{\tanh\zeta_1}{\mathrm{sech}^2\zeta_1}\right)$$
$$\left.\times\left\{\frac{1}{2}\eta_1(1-4\zeta_1\tanh\zeta_1)\mathrm{sech}^2\zeta_1\right.\right.$$

$$+\frac{(1+m)}{2ac\sigma_0}\gamma_1(2\zeta_1\,\mathrm{sech}^2\zeta_1-\tanh\zeta_1)\Big\}\Big]\Big]\tan\varphi$$
$$+\Lambda_2\Big[C_{Dw2}\Big\{\frac{(2n_1+1)(2n_1^2+10n_1+3)}{(n_1+1)(4n_1+1)}\Big(\frac{u_c^*}{u_0}\Big)+1\Big\}^2$$
$$+4\Big(\frac{u_0}{u_c^*}\Big)\Big[\frac{4n_1(2n_1+1)^2(n_1^2+5n_1+2)}{(4n_1+1)^2}\Big(\frac{u_c^*}{u_0}\Big)^2$$
$$+\frac{(3n_1+1)(2n_1+1)^2}{(4n_1+1)^2}(\lambda_1)^{-2}\Big(\frac{u_c^*}{u_0}\Big)^4\Big\{\frac{3(3n_1+1)}{n_1+1}$$
$$+2(n_1+1)(\lambda_1)^{(n_1-1)/2n_1}\Big(\frac{u_c^*}{u_0}\Big)^{2/n_1}$$
$$+\frac{4n_1(n_1+1)}{(3n_1+1)}(\lambda_1)^{-(n_1+1)/n_1}\Big(\frac{u_c^*}{u_0}\Big)^2\Big\}+\frac{(2n_1+1)(3n_1+1)}{4n_1+1}\Big(\frac{u_c^*}{u_0}\Big)^2$$
$$+\frac{1}{\sqrt{2}}\Big(\frac{d}{al_\delta}\Big)\Big]+(1+2\sqrt{2})\Big(\frac{d}{al_\delta}\Big)\Big]\tan\varphi. \quad\cdots\cdots(102)$$

As described above, it can be seen that the criterion for scour in the region of $\xi_c>\xi\geq 2a^2$, the zone of established flow, is expressed by the following relationship for both cases of the laminar and the turbulent boundary layers.

$$\frac{u_c^{*2}}{(\sigma/\rho-1)gd\tan\varphi}=\frac{4}{3\phi_i}. \quad (i=5,\ 6,\ 7,\ 8),\cdots\cdots(103)$$

in which

$$\phi_i=\phi_i\{u_c^*d/\nu,\ u_c^*/u_0\}.\cdots\cdots(104)$$

In calculating these equations, it is necessary to consider the relation between the friction coefficient C_f and the Reynolds number u_0L/ν as described already. Fig. 23 presents the relation between C_f and u_0L/ν, and the solid lines in the figure are the relations expressed by Eqs. (13) and (20) neglecting the second terms in brackets on the right.

Now consider the range of the Reynolds number u_0L/ν from 6×10^3 to

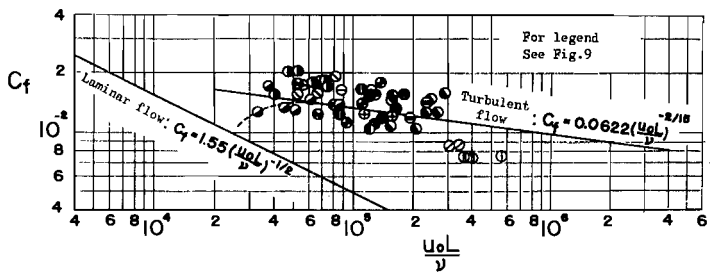

Fig. 23. Relation between C_f and u_0L/ν in region of $\xi>2\alpha^2$.

10^7, and it will be adequate to calculate Eqs. (103) and (104) for the ranges of u_c^*/u_0 from 0.1 to 0.06 for the laminar boundary layer and from 0.09 to 0.06 for the turbulent boundary layer respectively. By applying the values of n_1 and λ_1 used in the analysis of the boundary layer, that of σ_0 corresponding to the value of c as described already and $m=0.1$ to Eqs. (103) and (104), the theoretical curves for the criterion for scour can be calculated as shown in Fig. 24. In the figure, Iwagaki's theoretical curve for the critical tracive force[7] is shown for comparison. Besides, in the case of the laminar boundary layer the value of $u_c^{*2}/(\sigma/\rho-1)gd\tan\varphi$ tends to approach 0.056 independently of the values of u_c^*/u_0 when the value of u_c^*d/ν becomes lesser than unity and the value is equal to 0.056 in the range where the Stokes law can be applied to the drag coefficient.

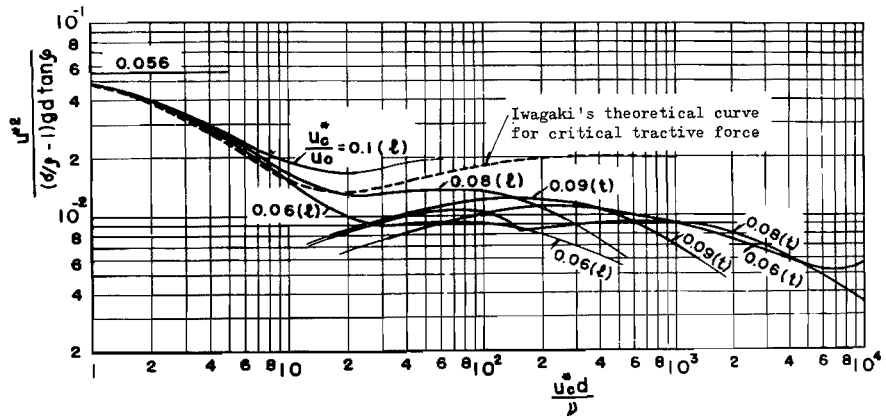

Fig. 24. Dimensionless expression of criterion for scour in zone of established flow obtained by the theory.

From the above descriptions and the theoretical results shown in Figs. (21) and (24), it is clear that the criterion for scour from wall jets is presented by the three parameters, $u_c^{*2}/(\sigma/\rho-1)gd\tan\varphi$, u_c^*d/ν and u_c^*/U or u_c^*/u_0, and especially by comparing the results with the critical tracitve force and the criterion for scour from flows downstream end of a smooth bed[9], it is found that a parameter u_c^*/U or u_c^*/u_0 should be added. Although this fact is based on the boundary layer growth, the tendencies of change of the theoretical curves are very complicated as is seen in Figs. (21) and (24), and the effect of the parameter u_c^*/U or u_c^*/u_0 may not be large, especially in the region of established flow. It is also concluded

from the comparison between the above theoretical curves and those for the critical tractive force that the criterion for scour from wall jets is presented by the lesser critical shear velocity than that for the critical tractive force in the region of sufficiently large u_c^*d/ν.

4) Theoretical consideration for the third region where the study of wall jets cannot be applied

Since the theoretical results of the wall jet described in the second chapter can not be directly applied to estimate the characteristics of flows in this region owing to the existence of a free water surface, the characters of flows should be dependent only on the result that the maximum velocity of the flow will more rapidly derease with a distance than that in free turbulent jets. To consider mathematically the criterion for scour in the region would be impossible. Hence, the relation between the criterion for scour in the region and that in the two regions described already is considered by the procedure of dimensional analysis based on the results shown in Fig. 3.

As described already, the most important parameter in the criterion for scour is the shear velocity along the bed. Instead of the shear velocity, maximum velocity of flows will approximately be applied. It is clear from the results shown in Fig. 3 that the characters of the maximum velocity expressed by $\bar{u}_0/U$ in dimensionless form, in the region of $\xi_c<\xi$ are closely connected with the ratio of the tail water depth to the length of an apron expressed by h_0/L, and furthermore, the flow should approach the uniform flow at a long distance from an outlet.

In the region of $\xi<\xi_c$, the tail water depth has been essentially ignored in the boundary layer growth and the criterion for scour as described already. Then, if the length of an apron and the water temperature are given, the velocity of water jets under the criterion for scour can surely be decided. Considering the fact and the characters of the flow described above, the criterion for scour in the region of $\xi>\xi_c$ will approximately be expressed by the following relation in connection with the theoretical results for the criterion in the former two regions.

$$U/U_w=f(h_0/L), \quad \cdots\cdots(105)$$

in which U is the velocity of an outlet already defined under the criterion for scour in the case when the length of an apron L, the characters of sand gravels, the opening of the outlet and the water temperature are given, U_w

the virtual velocity of a wall jet corresponding to U under the same conditions, and $f(h_0/L)$ which is the function of h_0/L and which should be decided only experimentally.

Furthermore, the more precise consideration for the criterion may require a clarification of the characteristics of flows in the region, although it may be very difficult to disclose theoretically the criterion due to very complicated phenomena associated with the development of local and gross turbulence. From the above assumption, if the relation expressed by Eq. (105) is considered and can be verified by the experimental results, the criterion for scour in the region may be estimated on the basis of the theoretical results for the two regions already described.

(2) Experiments on the criterion for scour resulting from wall jets

In order to consider the actual phenomena of the criterion for scour based on the theoretical considerations already described, the experiments for the three regions were performed.

1) Experimental apparatus and procedures

(i) Experimental water tank: With the experimental water tank described in the second chapter, the experiments on the criterion for scour were carried out by constructing the model apron on the upstream side and spreading sand gravels on the bed downstream of the apron. The length of the apron was determined for the three regions already described in connection with the opening of an outlet, and the aprons were made of a smooth brass plate. Control of discharge was done by installing the sluice valves in pipes connected with the experimental water tank. Velocities of the outlet were measured by the Pitot-tube with an outer diameter of 0.200 cm.

(ii) Properties of sand gravels used: The properties of the sand gravels used in the experiments are shown in Table 1. In order to take uniform sand gravels, the mean values of the sieve sizes, 0.03~0.06 cm, 0.06 ~0.12 cm, 0.12~0.25 cm, 0.25~0.50 cm, 0.50~-0.70 cm, 1.5~2.0 cm and 2.0 2.5 cm were used respectively. The values of the frictional angle of sand gravels, denoted by φ, the shape factor defined by $c/\sqrt{ab}$, in which a, b and c are the maximum, intermediate and minimum mutually perpendicular axes of a sand gravel, and the numbers of sand gravels exposed per unit area shown in Table 1 were measured by the same method as used by the

Table 1. Properties of used sand gravels and steel spheres.

Grain diameter d cm	Specific gravity σ/ρ	$\tan\varphi$	Number of sands and gravels exposed per unit area cm^{-2}	Shape factor $c/\sqrt{ab}$
0.0450	2.479	0.790	191	0.624(0.276～0.876)
0.0900	2.507	0.984	64.9	0.634(0.198～0.889)
0.185	2.512	1.045	23.7	0.651(0.354～0.904)
0.375	2.527	1.036	8.96	0.671(0.328～0.924)
0.600	2.528	1.082	3.78	0.678(0.600～0.917)
1.75	2.661	1.041	0.811	0.562(0.316～0.869)
2.25	.2.660	1.019	0.572	0.571(0.346～0.835)
0.332 (sphere)	7.675	1.021	9.70	1

author[9]

Besides, as an example for comparing the differences of shapes and specific gravities of sand gravels, the experiments for the zone of established flow were performed by using a steel sphere, shown in Table 1.

(iii) Experimental procedures : The relation between the velocity of an outlet and the rate of sediment transportation, expressed by the numbers of sediments, at or near the downstream end of the apron were measured by setting the sand gravels on the bed downstream of the apron and controlling the discharge of flow. But the criterion for scour in the third region where the study on wall jets may not be applied, was decided on the intuition of an observer because the accurate measurement of the rate of sediment transportation was very difficult owing to the development of complicated turbulence.

2) Experimental results and considerations

In the following, the experimental results obtained above are compared with the theoretical results for the three regions respectively.

(i) Considerations for the zone of flow establishment : From the experimental data in this region, some examples of the relations between the ratio, denoted by p_0 %/s, of the rate of sediment transportation, which is expressed by the numbers of sediments, to the numbers of sand gravels exposed per unit area, which was proposed by the author in the preceding paper[9], and the velocity of jets can be obtained as is shown in Fig. 25.

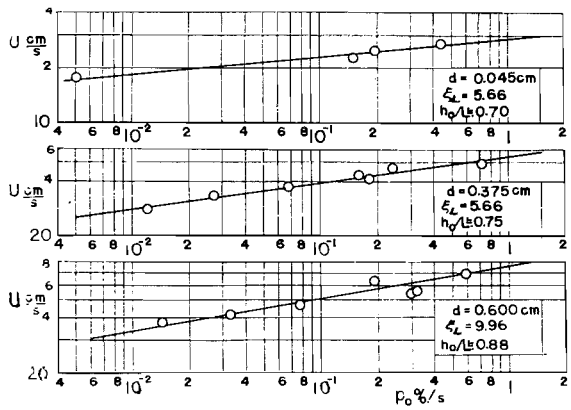

Fig. 25. Variations in rate of sediment transportation, expressed by p_0 %/s, with velocity of outlets.

Applying the value $p_0=0.5$ %/s, which was determined by the author in the previous paper, to the criterion for movement of sand gravels, the velocity of the outlet corresponding to the value can be obtained from the results shown in Fig. 25. Obtaining the value of C_f corresponding to the

Table 2. Experimental results for the criterion for scour in region of flow establishment.

d cm	L/D	U cm/s	u_c^*/U	u_c^* cm/s	u_c^*d/ν	$u_c^{*2}/(\sigma/\rho-1)gd\tan\varphi$
0.0450	5.66	27.4	0.0599	1.64	6.97	0.0524
0.0900	〃	31.1	0.0588	1.83	15.5	0.0279
0.185	〃	38.0	0.0573	2.18	38.0	0.0166
0.375	〃	50.0	0.0556	2.78	97.8	0.0133
0.600	〃	70.0	0.0538	3.77	212	0.0146
1.75	8.16	135.0	0.0476	6.43	901	0.0139
2.25	〃	146.0	0.0472	6.89	1242	0.0127
0.0450	9.96	29.8	0.0556	1.65	7.04	0.0532
0.0900	〃	36.7	0.0543	1.99	16.9	0.0296
0.185	〃	41.3	0.0534	2.21	38.5	0.0171
0.375	〃	53.2	0.0519	2.76	97.4	0.0132
0.600	〃	69.4	0.0507	3.52	198	0.0128

Reynolds number UL/ν, which is calculated from the value of U, the length of an apron L and the kinematic viscosity ν, from the results shown in Fig. 20, and estimating the critical shear velocity u_c* from the results, the values of $u_c{}^{*2}/(\sigma/\rho-1)gd\tan\varphi$ and $u_c{}^*d/\nu$ can be calculated. In this case, the relation shown in Fig. 20 by the chain line was applied to estimate the value of C_f in the case when the value of UL/ν became about 2×10^4. The relationship between C_f and UL/ν close to the above value has not been clarified yet. Since, however, this corresponds to the case when the size of sand grain is equal to about 0.045 cm, these many differences will not remain in practical problems. The experimental results obtained above are

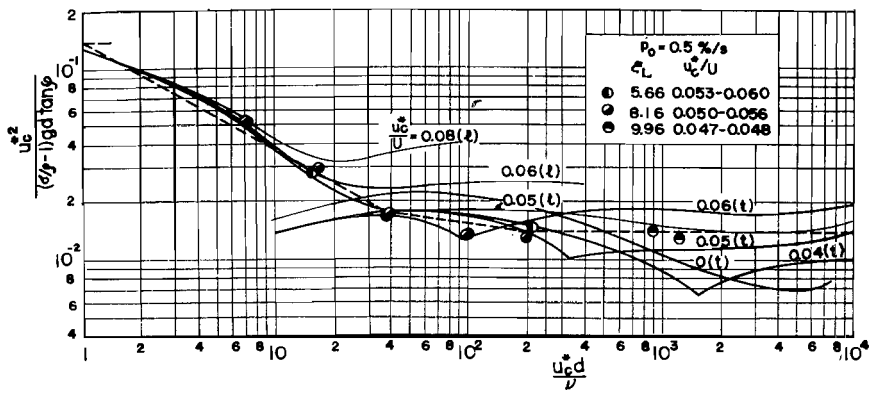

Fig. 26. Comparison of experimental results and theoretical curves for criterion for scour in region of flow establishment.

shown in Table 2. Fig. 26 presents the comparison of the theoretical curves for the criterion and the experimental results shown in Table 2. The theoretical curves in the figure were decided as follows. By introducing the sheltering coefficient proposed by Iwagaki[7] into Eq. (63), it can be written as

$$\frac{u_c{}^{*2}}{(\sigma/\rho-1)gd\tan\varphi}=\frac{4}{3\varepsilon\phi_i},\quad (i=1,\ 2,\ 3,\ 4)\cdots\cdots\cdots\cdots\cdots(106)$$

in which ε is equal to 0.4 on the basis that the hydraulic mechanism for the sheltering coefficient may approximately agree with that in the case of the critical tractive force[7] and the criterion for scour at the downstream end of a smooth bed[9] Since the theoretical curves are not expressed by one curve with the parameter $u_c{}^*/U$ because the transition of the boundary

layer from laminar to turbulent is not clear, the complete comparison of the theoretical curves and the experimental results cannot be made. In spite of these many assumptions, the theoretical curves agree well with the experimental results, and it seems that the effects of the parameter u_c*/U on the criterion do not come within the range of the experiments.

(ii) Considerations for the zone of established flow: The experiment-

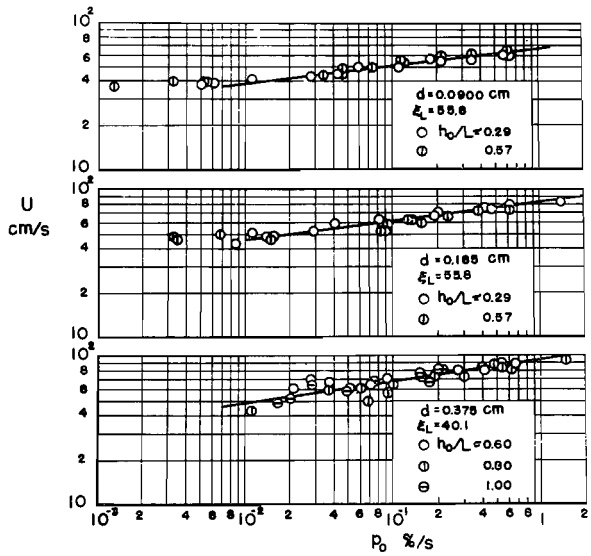

Fig. 27. Variations in rate of sediment transportation, expressed by p_0 %/s, with velocity of outlets in case of sand grains.

al results arranged as described above are shown in Figs. 27, 28 and 29. Fig. 27 shows some examples of the experimental results obtained by using the sand grains, Fig. 28, by using the gravels and Fig. 29, by using the steel spheres. As is shown in Fig. 25, the variations in

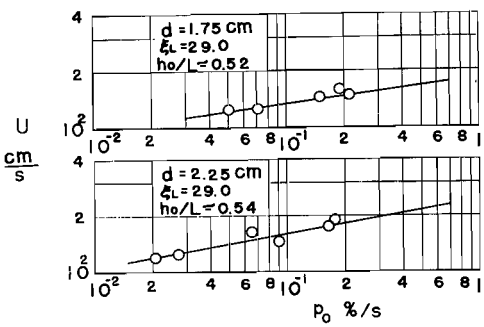

Fig. 28. Variations in rate of sediment transportation, expressed by p_0 %/s, with velocity of outlets in case of gravels.

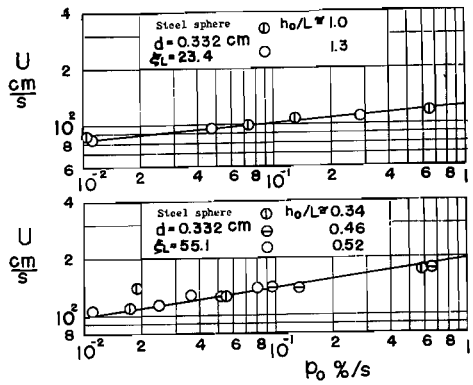

Fig. 29. Variations in rate of sediment transportation, expressed by p_0 %/s, with velocity of outlets in case of steel spheres.

the velocity of the outlet U with the rate of sediment transportation p_0 %/s are not great enough, and especially for the region, all of the experimental data for the case of $h_0/L<0.288$ obtained from Fig. 4 are expressed by a curve when the water temperature is constant, in spite of the expression with the parameter of h_0/L. This fact will be the natural outcome to be expected from the characteristics of wall jets described in the second chapter. The limit of applicability will be explained in the considerations of the next region.

Calculating the velocity u_0 by Eq. (6) by applying the definition for the criterion for movement of sand gravels, expressed by $p_0=0.5$ %/s, to these experimental results as described already, and estimating the critical shear velocity by using Fig. 23 instead of Fig. 20, the final results can be obtained as shown in Table 3. Fig. 30 represents the comparison between the

Table 3. Experimental results for criterion for scour in region of established flow.

d cm	L/D	U cm/s	u_c^*/u_0	u_c^* cm/s	$u_c^* d/\nu$	$u_c^{*2}/(\sigma/\rho-1)gd\tan\varphi$
0.0450	23.4	32.6	0.0788	1.713	8.16	0.0569
0.0900	〃	44.7	0.0823	2.45	22.9	0.0457
0.185	〃	53.4	0.0850	3.03	58.7	0.0318
0.375	〃	64.0	0.0839	3.42	138.0	0.0227
0.600	〃	92.2	0.0821	5.05	312	0.0275
1.75	29.0	168	0.0774	7.76	1086	0.0203
2.25	〃	213	0.0761	9.70	1747	0.0252
0.0450	40.0	39.0	0.0859	1.704	7.72	0.0562
0.0900	〃	53.5	0.0836	2.30	21.7	0.0403
0.185	〃	66.5	0.0823	2.78	54.0	0.0270

0.375	〃	80.5	0.0813	3.33	130.5	0.0191
0.600	〃	106.6	0.0801	4.39	271	0.0208
0.0900	40.1	49.9	0.0832	2.12	22.8	0.0342
0.185	〃	67.4	0.0814	2.80	60.7	0.0274
0.375	〃	86.7	0.0806	3.56	158.9	0.0218
0.0450	55.8	50.8	0.0822	1.807	9.58	0.0633
0.0900	〃	61.2	0.0816	2.16	22.9	0.0357
0.185	〃	76.0	0.0803	2.64	53.4	0.0243
0.375	〃	103.6	0.0785	3.52	156.2	0.0213
0.600	〃	130.0	0.0770	4.34	305	0.0194
0.322 (steel sphere)	23.4	115.2	0.0809	6.22	199.1	0.0179
〃	55.1	180.0	0.0765	6.01	193.4	0.0167

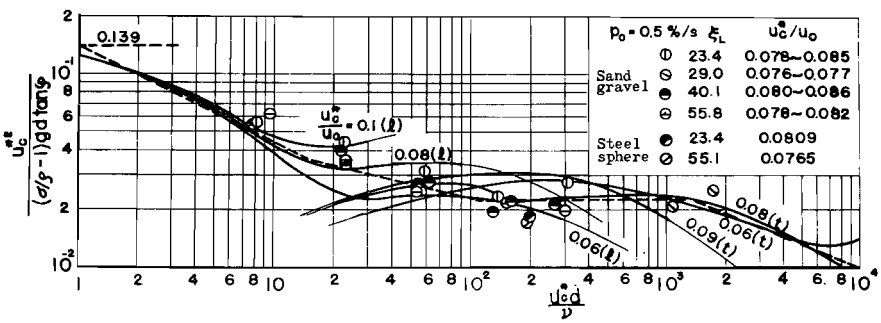

Fig. 30. Comparison of experimental results and theoretical curves for criterion for scour in region of established flow.

theoretical curves for the criterion and the experimental results shown in Table 3. The theoretical curves for the criterion in the figure are expressed in the form of

$$\frac{u_c^{*2}}{(\sigma/\rho-1)gd\tan\varphi}=\frac{4}{3\varepsilon\phi_i},\quad (i=5,\ 6,\ 7,\ 8)\cdots\cdots\cdots\cdots\cdots\cdots(107)$$

in which ε is equal to 0.4 as described already. As described in the case of Fig. 26, the theoretical curves are not expressed by one curve with the parameter u_c^*/u_0, so the complete comparison with the experimental results can not be made. It is clear, however, that the comparison is well and especially the experimental results obtained by using the steel

spheres agree well also with the theoretical curves. It will be deduced from the fact that the effects of the shape factor of a sand gravel on the criterion for scour expressed by the relationship between $u_c^{*2}/(\sigma/\rho-1)gd\tan\varphi$ and u_c^*d/ν are not very great, as concluded in the preceding paper by the author[9]. if the shape factor is of the range from 0.56 to 1. And it is found that the deviations in the theoretical curves especially the deviations in $u_c^{*2}/(\sigma/\rho-1)gd\tan\varphi$ at a given value of u_c^*d/ν with the parameter u_c^*/u_0, are in the same order as those in the experimental results, and the fact that the effect of the parameter u_c^*/u_0 on the criterion for scour is not clear and not very great, may be verified by the experimental results. The conclusion based on this fact should be decided on the basis of the model experiments with a large scale or the field observations for an actual outlet because the range of values of u_c^*/u_0 in the experiments are not sufficient.

Taking the comparison of the results shown in Fig. 26 and those shown in Fig. 30, it is clear that the variations in the theoretical curves with the parameter u_c^*/U in the former case are greater than those with the parameter u_c^*/u_0 in the latter case, but both theoretical curves show closely the same tendency close to $u_c^*d/\nu=10^3$. For the range of $u_c^*d/\nu=10^3$, however, it seems that the former changes are complicated with the parameter u_c^*/U, the value of $u_c^{*2}/(\sigma/\rho-1)gd\tan\varphi$ is nearly constant for the change of u_c^*d/ν, and on the contrary, the value in the latter decreases with the parameter u_c^*d/ν. In order to clarify the comparison of the theoretical curves and the experimental results in this range, it is necessary to perform the model test having a large scale or the field observations because the size of gravels in the range becomes larger than 5 cm approximately. In particular, although the theoretical curve of $u_c^*/u_0=0.06$ tends to separate from that of $u_c^*/u_0=0.08$ at or near the value of which $u_c^*d/\nu=6\times10^3$, the detail considerations for the theoretical curves can not be made, since the Reynolds number in calculating the curve of $u_c^*/u_0=0.08$ has become the critical Reynolds number of a sphere close to the value of u_c^*d/ν above mentioned. Therefore, the considerations should be applied only in the experiments.

(iii) Considerations for the third region where the study of wall jets is not applied: Based on the consideration on the criterion for scour described already, the relation of Eq. (106) can be verified by the experimental

results for this region. As described already, the decision for the criterion for scour in this region was made on intuition of an observer by an assumption, so the experimental data may scatter. But the discrepancy in the hydraulic phenomenon of the criterion for scour may not exist. Fig. 31 is the result considered for the relation expressed by Eq. (105), based on the above experimental results. It is clear from the results, that, for larger values of h_0/L than a certain one the velocity of an outlet agrees with the virtual velocity of a wall jet, which was defined already, in spite of the changes of ξ_L, D and d. Therefore, the region corresponds to that already described.

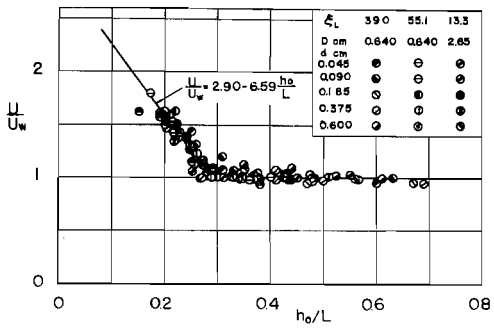

Fig. 31. Relation between U/U_w and h_0/L.

On the other hand, the value of U/U_w increases rapidly with the decrease of the value of h_0/L in the case where the value of h_0/L is lesser than the critical one. The region is to be considered in this section. It will be seen from the results shown in Fig. 31 that the relation between the ratio, which is expressed by U/U_w, of the velocity of an outlet to the virtual velocity of a wall jet and that, which is expressed by h_0/L, of the tail water depth to the length of an apron can be presented by only one curve in spite of the changes of the opening of an outlet, the ratio of the length to the opening and the size of sand gravels in a vast range. And it may be concluded from the fact that the relation of Eq. (105) obtained by means of a dimensional analysis with the aid of the theoretical considerations for the criterion for scour in the two regions described already, is practically correct.

Now, expressing the relation between U/U_w and h_0/L by the straight line shown in Fig. 31, within the range of the experiments, the relation can be written as

$$U/U_w = 2.90 - 6.59(h_0/L). \quad \cdots\cdots\cdots\cdots\cdots\cdots\cdots\cdots (108)$$

In the above equation, calculating the value of h_0/L at $U/U_w = 1$, the value is equal to 0.288, that is $h_0/L = 0.288$. It is very interesting to note that the value agrees with the limit of applicability of the theoretical con-

sideration on wall jets described in the second chapter. As is seen clearly from Eq. (108), the influence of the tail water depth on the criterion for scour appears in the case where the value of h_0/L is lesser than 0.288. And Eq. (108) describes the fact that the more tail water depth decrease, the more velocity of an outlet is needed to move the sand gravels at or near the downstream end of an apron.

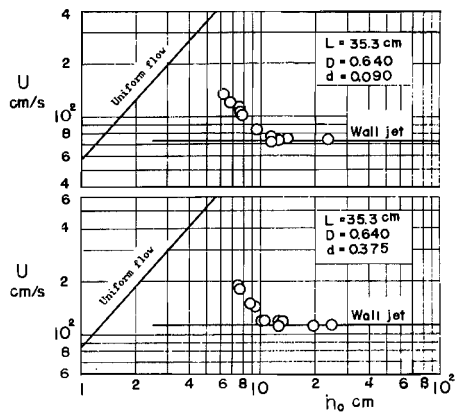

Fig. 32. Relation between velocity of outlets and tail water depth under criterion for scour.

Besides, the flow in the third region should approach the uniform flow at a long distance from the outlet, so in order to consider the above inference, the relation between the velocity of outlets and the tail water depth is shown in Fig. 32. It is seen from the figure that the experimental data soon approach the relation corresponding to the uniform flow, but the nature of the approach cannot be made clear within the range of the experiments.

(3) Empirical formulas of the criterion for scour and considerations for determining the length of an apron required for maintenance of an outlet

In this article, an empirical formula for the criterion for scour from flows downstream of an outlet and that for determining the length of an apron under the criterion for scour are proposed, based on both the results of the theoretical considerations and the experiments described above. The design charts available to derive the length of an apron are developed. The Bligh formula and the formula proposed at Iowa University are discussed in comparison with the author's formula. Moreover, some practical examples for determining the length of an apron are described and some considerations are briefly made on the design of aprons.

1) Empirical formulas

In order to discuss the criterion for scour from flows downstream of an outlet, the results shown in Figs. 26 and 30 are inadequate for practi-

cal purposes, so it is necessary to rewrite an empirical formula in simple form. For the purpose, an empirical formula for the criterion is proposed as follows.

(i) Empirical formula for the region of $L/D \leq 2a^2$ $(=10.4)$: In this case, the apron is in the zone of flow establishment. Now, expressing the relation between $u_c{}^{*2}/(\sigma/\rho-1)gd\tan\varphi$ and $u_c{}^*d/\nu$, shown in Fig. 26, by the broken line, by neglecting the influence of $u_c{}^*/U$, the lines can be expressed by the following empirical formula.

$$\left.\begin{aligned} R^*\geq 1330\ ; \quad & u_c{}^{*2}=0.0140\{(\sigma/\rho-1)g\tan\varphi\}d, \\ 286\leq R^*\leq 1330\ ; \quad & =0.0391\{(\sigma/\rho-1)g\tan\varphi\}^{13/14}\nu^{1/7}d^{11/14}, \\ 3.68\leq R^*\leq 286\ ; \quad & =0.216\{(\sigma/\rho-1)g\tan\varphi\}^{7/9}\nu^{4/9}d^{1/3}, \\ R^*\leq 2.68\ ; \quad & =0.139\{(\sigma/\rho-1)g\tan\varphi\}d, \end{aligned}\right\} \quad \cdots\cdots(109)$$

in which

$$R^*=\{(\sigma/\rho-1)g\tan\varphi\}^{1/2}d^{3/2}/\nu. \quad \cdots\cdots(110)$$

Further, simplifying the above relationships by using the values, $\sigma/\rho=2.65$, $\tan\varphi=1$, $\nu=0.01\ \mathrm{cm^2/s}$ (at 20.3°C) and $g=980\ \mathrm{cm^2/s}$, the results can be reduced to

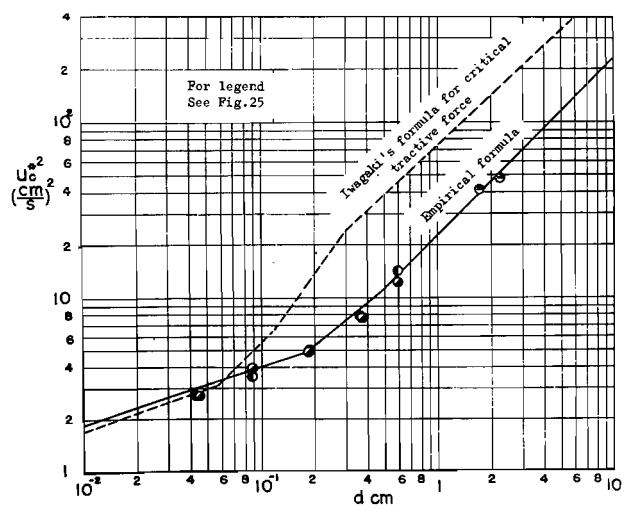

Fig. 33. Graphical representation of empirical formula for zone of flow establishment.

$$\left.\begin{array}{rll} d\geq 0.478\ \text{cm}\ ; & u_c{}^{*2}=22.6d\ \text{(cm/s)}^2, & \\ 0.172\leq d\leq 0.478\ ; & =19.3d^{11/14}, & \\ 0.00763\leq d\leq 0.172\ ; & =8.73d^{1/3}, & \\ d\leq 0.00763\ ; & =225d, & \end{array}\right\}\cdots\cdots\cdots\cdots\cdots\cdots(111)$$

in which d is in cm and $u_c{}^{*2}$ in $(\text{cm/s})^2$.

Fig. 33 is the graphical representation of Eq. (111), and the Iwagaki formula[7] for the critical tractive force is shown in the figure for comparison.

(ii) Empirical formula for the region of $2\alpha^2\leq L/D<\xi_0$: In this case, the apron is in the zone of established flow. Expressing the relation between $u_c{}^{*2}/(\sigma/\rho-1)\,gd\tan\varphi$ and $u_c{}^*d/\nu$, shown in Fig. 30, by the broken lines, the empirical formula can be written as

$$\left.\begin{array}{rll} 9050\leq R^*\leq 76400\ ; & u_c{}^{*2}=0.464\{(\sigma/\rho-1)g\tan\varphi\}^{5/6}\nu^{1/3}d^{1/2}, & \\ 670\leq R^*\leq 9050\ ; & =0.0223\{(\sigma/\rho-1)g\tan\varphi\}d, & \\ 79.6\leq R^*\leq 670\ ; & =0.0947\{(\sigma/\rho-1)g\tan\varphi\}^{8/9}\nu^{2/9}d^{2/3}, & \\ 2.68\leq R^*\leq 79.6\ ; & =0.207\{(\sigma/\rho-1)g\tan\varphi\}^{4/5}\nu^{2/5}d^{2/5}, & \\ R^*\leq 2.68\ ; & =0.139\{(\sigma/\rho-1)g\tan\varphi\}d, & \end{array}\right\}\cdots(112)$$

In Fig. 30, the experimental data only exist near $u_c{}^*d/\nu=2\times10^3$, so the comparison of the theoretical curves and the experimental results for the range of larger values of $u_c{}^*d/\nu$ can not be made. In proposing the empirical formula, therefore, the considerations for the range should be questioned. Based on the above consideration and the fact that the theoretical curves for the criterion in the ranges of $2\times10^2<u_c{}^*d/\nu<8\times10^3$ agree well with the experimental results in spite of the variations in the parameter $u_c{}^*/u_0$, the empirical formula has been proposed. From this, although the limit of applicability of the empirical formula has been presented by $u_c{}^*d/\nu=8\times10^3$, which corresponds to $R^*=76400$, the detail conclusion for the limit should depend upon the field observations in the future.

Making a formula which corresponds to Eq. (111) by using the practical values described already, the result can be reduced to

$$\left.\begin{array}{rll} 1.72\leq d\leq 7.12\ \text{cm}\ ; & u_c{}^*=47.3d^{1/2}\ \text{(cm/s)}^2, & \\ 0.303\leq d\leq 1.72\ ; & =3.61d, & \\ 0.0730\leq d\leq 0.303\ ; & =24.2d^{2/3}, & \\ 0.00763\leq d\leq 0.0730\ ; & =12.1d^{2/5}, & \\ d\leq 0.00763\ ; & =225d. & \end{array}\right\}\cdots\cdots\cdots\cdots\cdots\cdots(113)$$

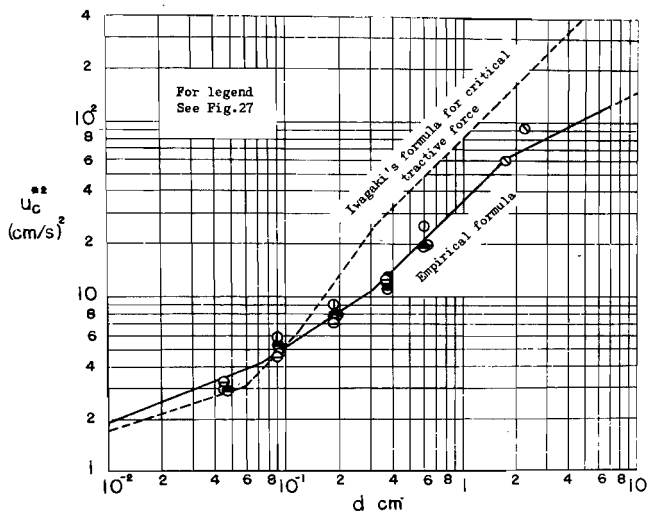

Fig. 34. Graphical representation of empirical formula for zone of established flow.

Fig. 34 shows the graphical representation of the above equation. In the figure, the theoretical curve for the critical tractive force by Iwagaki is shown for comparison as done in Fig. 33. It is clear from both results shown in Figs. 33 and 34 that the criterion for scour from flows downstream of an apron is presented by a lesser critical shear velocity than that in the critical tractive force in the range of sufficient large-size sand gravels. This fact is similer to that resulting from flows at the downstream end of a smooth bed described in the preceding paper[9].

(iii) Empirical formula for the region of $L/D>\xi_e$: The criterion for scour has been expressed by Eq. (108) in connection with the results for the other two regions described already. To express the criterion by the shear velocity may be generally difficult because the relationship for the resistance law of flow in the region has not yet been clarified. However, the expression of Eq. (108) may rather conveniently be applied to practical problems, so the author will propose the relation expressed by Eq. (108) without any modification for the empirical formula for the criterion in the region.

2) Considerations on the design of the length of an apron

(i) Empirical formula for determining the length of an apron: Inserting the resistance law of flow in those regions into the relationships

for the criterion for scour described above and transforming these relationships, the relations expressing the length of an apron under the criterion for scour can be obtained as follows:

a) Formula for $L/D \leq 10.4$: Inserting the resistance law in laminar boundary layers and the Blasius law shown in Fig. 20 into the empirical formula expressed by Eq. (109), the dimensionless length of an apron can finally be written as

$$
\left.
\begin{aligned}
&R^* \geq 1330\ ; \\
&\frac{L}{D} = 37.5\left(\frac{UD}{\nu}\right)^{-1}\left\{\frac{U^2}{(\sigma/\rho-1)gd\tan\varphi}\right\}^{5}, \\
&286 \leq R^* \leq 1330\ ; \\
&\quad = 0.220\left(\frac{d}{D}\right)^{65/9}\left(\frac{UD}{\nu}\right)^{-2/7}\left\{\frac{U^2}{(\sigma/\rho-1)gd\tan\varphi}\right\}^{65/14}, \\
&2.68 \leq R^* \leq 286\ ; \\
&\quad = 0.000434\left(\frac{d}{D}\right)^{20/9}\left(\frac{UD}{\nu}\right)^{11/9}\left\{\frac{U^2}{(\sigma/\rho-1)gd\tan\varphi}\right\}^{35/9} \quad \text{(turbulent)}, \\
&\quad = 0.0288\left(\frac{d}{D}\right)^{8/9}\left(\frac{UD}{\nu}\right)^{-1/9}\left\{\frac{U^2}{(\sigma/\rho-1)gd\tan\varphi}\right\}^{14/9} \quad \text{(laminar)}, \\
&R^* \leq 2.68\ ; \\
&\quad = 0.0691\left(\frac{UD}{\nu}\right)^{-1}\left\{\frac{U^2}{(\sigma/\rho-1)gd\tan\varphi}\right\}^{2}
\end{aligned}
\right\} \quad \cdots\cdots (114)
$$

In the above equation, both expressions of the laminar and the turbulent boundary layers for the same range of the value of R^* are necessary to calculate for practical purposes because the critical Reynold number in transition from laminar to turbulent and the characters of the transition have not yet been clarified. According to Fig. 20, the case where the transition is questionable, is close to $u_c{}^*d/\nu \approx 25$ in practical problems, so the empirical formulas for the region have been presented by the relationships obtained by using the two resistance laws for the above boundary layers. Then, the application of the relationships to practical use should be attempted as is explained below. If the value of R^*, which expressed by Eq. (110), calculated from the characters of sand gravels and the water temperature, is in the region of $2.68 \leq R^* \leq 286$, the length of an apron corresponding to the given characters of an outlet is obtained by using the two formulas for the region expressed by Eq. (114). And, representing the values of the Reynolds number UL/ν obtained by the above results and the local

skin friction coefficient which is expressed by $C_f=2(u_c*/U)^2$ and calculated by using Eqs. (5) and (109) under the given codition, into Fig. 20, it may be concluded from the comparison of the results with the relations shown in Fig. 20 by the two solid and the broken lines, which relationship of the laminar or the turbulent boundary layer would be adaptable to the case.

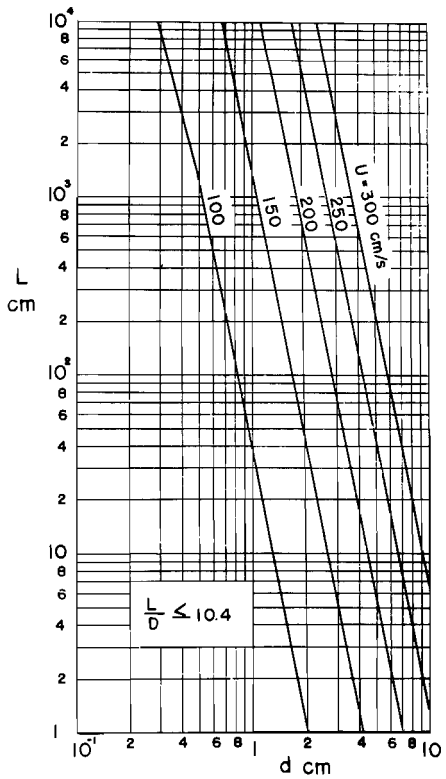

Fig. 35. Design chart for determining length of an apron under criterion for scour in case of $L/D\leq 10.4$.

Moreover, it is clear from Eq. (114) that the length of an apron under the criterion for scour is independent of the opening of an outlet in the case of large sand gravels and proportional to $U^9d^{-n'}$ in which n' is in the range from 5/3 to 5. Fig. 35 presents the relationship among the length of an apron under the criterion for scour, the size of sand gravels and the velocity of an outlet, obtained by using the same values as used in Eq. (111) into Eq. (114). From the design chart shown in Fig. 35, the desirable length of an apron under the criterion for scour can easily be obtained under the given conditions of the size of sand gravels and the velocity of an outlet. However, the range of applicability of the design chart is $L/D\leq 10.4$.

b) Formula for $10.4\leq L/D<\xi_c$: Putting the relations for the resistance law shown in Fig. 23 into Eq. (112) by the same procedure as described above, the relationship expressing the length of an apron under the criterion for scour in the region of $10.4\leq L/D<\xi_c$, corresponding to Eq. (114) can finally be reduced to

$$
\left.
\begin{aligned}
&9050 \leq R^* \leq 76400\ ; \\
&\qquad \frac{L}{D} = 0.614\left(\frac{d}{D}\right)^{5/16}\left(\frac{UD}{\nu}\right)^{3/16}\left\{\frac{U^2}{(\sigma/\rho-1)gd\tan\varphi}\right\}^{25/32}, \\
&670 \leq R^* \leq 9050\ ; \\
&\qquad = 10.60\left(\frac{UD}{\nu}\right)^{-1/8}\left\{\frac{U^2}{(\sigma/\rho-1)gd\tan\varphi}\right\}^{15/10}, \\
&79.6 \leq R^* \leq 670\ ; \\
&\qquad = 2.73\left(\frac{d}{D}\right)^{5/24}\left(\frac{UD}{\nu}\right)^{1/12}\left\{\frac{U^2}{(\sigma/\rho-1)gd\tan\varphi}\right\}^{5/6} \quad \text{(turbulent)}, \\
&\qquad = 21.9\left(\frac{d}{D}\right)^{8/45}\left(\frac{UD}{\nu}\right)^{-2/9}\left\{\frac{U^2}{(\sigma/\rho-1)gd\tan\varphi}\right\}^{32/45} \quad \text{(laminar)}, \\
&2.68 \leq R^* \leq 79.6\ ; \\
&\qquad = 1.317\left(\frac{d}{D}\right)^{3/8}\left(\frac{UD}{\nu}\right)^{1/4}\left\{\frac{U^2}{(\sigma/\rho-1)gd\tan\varphi}\right\}^{3/4} \quad \text{(turbulent)}, \\
&\qquad = 11.74\left(\frac{d}{D}\right)^{8/25}\left(\frac{UD}{\nu}\right)^{-2/25}\left\{\frac{U^2}{(\sigma/\rho-1)gd\tan\varphi}\right\}^{16/25} \quad \text{(laminar)}, \\
&\qquad R^* \leq 2.68\ ; \\
&\qquad = 16.11\left(\frac{UD}{\nu}\right)^{-2/5}\left\{\frac{U^2}{(\sigma/\rho-1)gd\tan\varphi}\right\}^{4/5}
\end{aligned}
\right\} \quad \cdots\cdots(115)
$$

Both expressions of the laminar and the turbulent boundary layers for the same range of the value of R^* in the above equations depend upon the same reason described above, and the procedure for the application of the relationships is also the same as in the former region by using only the value of the Reynolds number u_0L/ν, Eq. (6) and Fig. 23 instead of the value of UL/ν, Eq. (5) and Fig. 20 respectively. And it is clear from Eq. (115) that the length of an apron is proportional to $(U^2D)^{7/8}d^{-n'}$, in which n' is in the range from 5/8 to 15/16, in the case of considerable large-size sand gravels. Fig. 36 shows the design chart for determining the length of an apron in the region of $10.4 \leq L/D < \xi_c$, which is expressed by the relations among the length of an apron L, the size of sand gravels d and the quantity U^2D proportional to the momentum of flow at the outlet, based on the relationships expressed by Eq. (115). The necessary length of an apron for preventing the bed from scour can easily be estimated if the opening of an outlet, the velocity and the size of sand gravels are given. It should be mentioned, however, that the range of applicability of the relationships is the range where $L/D \leq 10.4$ and the ratio of the tail water depth

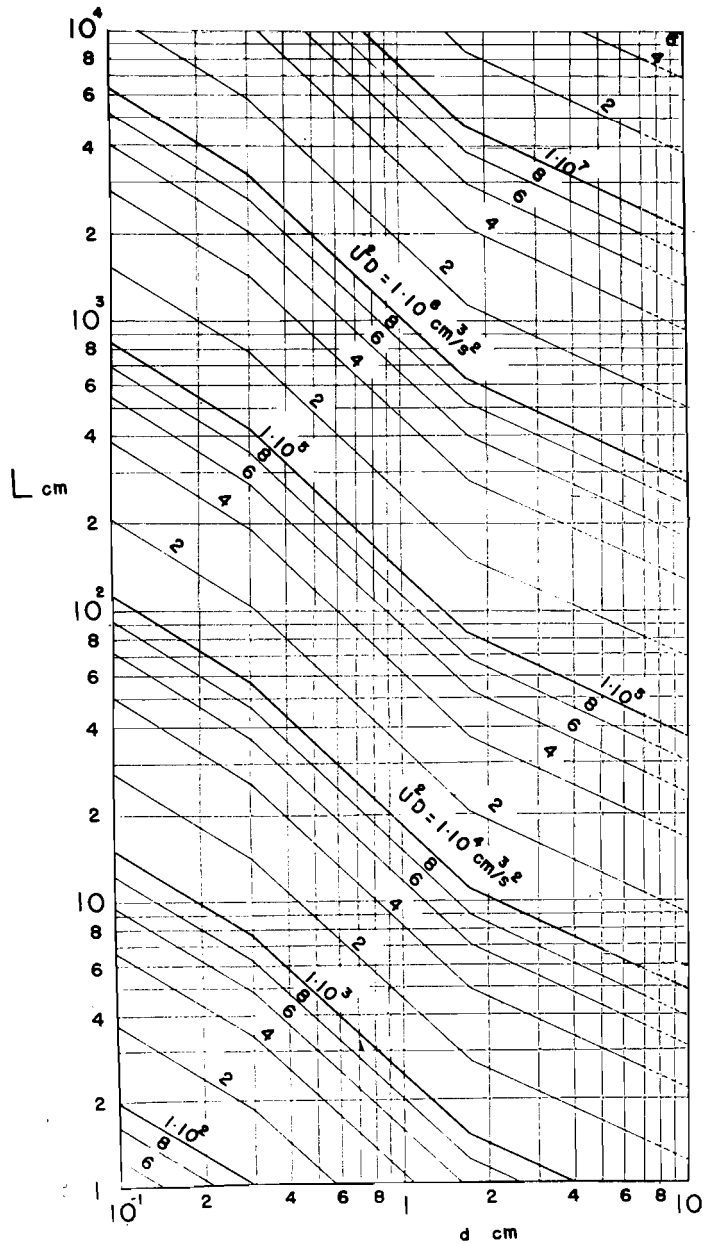

Fig. 36. Design chart for determining length of an apron under criterion for scour in case of $10.4 \leq L/D < \xi_c$.

to the length of an apron expressed by h_0/L is greater than 0.288.

c) Formula for $L/D>\xi_c$: As described already, the empirical formula for the criterion for scour in the region has been obtained in connection with the results in the former two regions, and expressed by Eq. (108). The use of the equation in practical problems is briefly explained below. Signification of Eq. (108) has already been presented. In order to estimate the length of an apron in the region, therefore, is necessary to solve simultanously both equations of Eq. (115), in which U in the equation is replaced by U_w, having the given condition for the opening, the velocity of an outlet, the characters of sand gravels, the tail water depth and the water temperature, and Eq. (108) by the length of an apron. For the purpose, the next procedure can generally be available. Represent the relation between $(U^2D)_w$ and L by using Eq. (115) or Fig. 36 under the given condition into the figure, calculate the following relation which is obtained from Eq. (108)

$$(U^2D)_w = U^2D/(2.90-6.59h_0/L)^2, \quad \cdots\cdots(116)$$

by using the given values of the tail water depth and U^2D. Show the relation in the same figure, or the required length of an apron will be estimated from the intersection of these curves. And the value of U_w in the figure is the velocity of a virtual wall jet defined already.

(iii) Considerations of former formulas for determining the length of an apron : As described in the introduction, the Bligh formula which is the only one for estimating practically the length of an apron at the present time, can be written as[1,2]

$$L' = 3\bar{c}\sqrt{h/3}\sqrt{q/7}, \quad \cdots\cdots(117)$$

in which L' is the overfall width of the hydraulic works protecting the bed against scour in m. This should be measured in a downstream direction from the fall, in which the erosion energy is generated, to the end of the rip-rap, pitching, or such like protecting works ; it being understood that the width must suffice to dissipate entirely the energy of the fall, so that no dangerous scour holes may form in the unprotected bed of a stream channel downstream of the protection, h and the height of the fall from the crest of a weir, or from the top of a shutter or a gate, down to the tail water level in m, q the discharge per unit length of a weir or a barrage in m^2/s, and $\bar{c}$ an empirical coefficient characteristic of materials

of a stream channel which was named by Bligh as the percolation factor, in so far as its capacity, or otherwise, of being eroded by action of flow is concerned.

This formula was found on the basis of the idea that the distance of the toe of a talus from the overfall would vary with the square root of the height of an obstruction above tail water, designated by h, with the square root of the unit flood discharge over the crest of a weir, denoted by q, and directly with $\bar{c}$, the percolation factor of the river sand. The formula, though more or less empirical, would give some results remarkably in consonance with actual values, and would, it is believed, form a valuable guide in practical design[2]

Since the critical considerations on the Bligh formula have been made by Minami[6] in detail, the author will not discuss the formula. Historically speaking, there is no doubt that the formula is questionable. It shoul be mentioned, however, that the formula is a very valuable empirical one, as it was proposed on the basis of the many results of field observations.

As described already, the Iowa formula[1] based on the results of laboratory experiments could possibly be cited for comparison with the Bligh formula. For the apron without piers, the formula is given by

$$L'' = qh_0/(h_0+h')^2, \quad \cdots\cdots (118)$$

in which L'' is the length of an apron without baffle-piers, h_0 the tail water depth and h' the effective head of a fall. Furthermore, the formulas for determining the length of an apron or width of rip-raps, pitching, or similar loose protections, were proposed, but these will be neglected in describing and considering because they have no relationship with the present study. Other examples of a general formula derived from model tests, such as formulas proposed by Veronese[4], Kohsla and Ahmad[5] as described already, may be cited, but these will not be presented here because the treatments based on the mechanism of local scour by the above authorities are not directly concerned with the present paper.

Although the relation between the former empirical formulas described above and the author's empirical formulas expressed by Eqs. (114), (115) and (116) should be considered, the quantitative comparison for both formulas cannot be described because the reductions of these formulas are different from each other. Then the qualitative comparisons presented as

follows:

Now, consider the relation between Eq. (115) and the Bligh formula. Since Eq. (117) explicitly excludes without the tail water depth, it will be supposed that the Bligh formula corresponds to the author's in the region of $h_0/L>0.288$. As described already, the relation expressed by Eq. (115) is closely related to $L\propto(qU)^{7/8}\ d^{-n'}$ in which $q=UD$, discharge of flow per unit width, $n'=5/8-15/16$. Then, expressing the velocity U by the head of water h' by introducing the discharge coefficient, the relation can be written as

$$L\propto(q/h')^{7/8}d^{-n'} \quad \cdots\cdots(119)$$

Supposing that the length L' expressed by Eq. (117) is nearly the same as the length L expressed by the above equation, it is clear from the comparison of both relations of Eqs. (117) and (119) that the power in the discharge q in Eq. (119) is twice as large as that in the Bligh formula, and contrarily, the power in the head of water is nearly the same. Moreover, Bligh proposed the coefficient for the influence of grain sizes of sand gravels on the required length of an apron and the relation between the length and the grain size was found. The qualitative tendency that the length of an apron decreases with the grain size is the same as in the author's formulas. Then, the fact that the influence of the grain size on the required length of an apron was introduced in the formula in any form should be rated high.

Subsequently, the relation between the author's formula and the Iowa formula is considered. Supposing that the length L expressed by Eq. (118) is the same as that in Eq. (119), the power in the discharge of flow in Eq. (118) is nearly equal to that in Eq. (119). For the special characteristics of Eq. (118), it is pointed out that the effect of the tail water depth on the required length is clearly considered and, on the contrary, that of the characters of sand gravels is neglected. Since it is not clear why the effects of the characters of sand gravels were not considered, the effect of the tail water depth is considered only below. In order to consider the effect, the case of $h'\geq h_0$ should be discussed. In the case of $h'/h_0\leq 1$, the length of an apron L'' decreases with the tail water depth for the given discharge, and contrarily, in the case of $h'/h_0>1$ the length increases with the tail water depth.

On the other hand, the author's formulas are independent of the tail water depth for the region of $h_0/L<0.288$, so the comparison of the formulas with that of Iowa University can not be made, therefore, only the case of $h_0/L>0.288$ is considered. As described in (ii), the length of an apron becomes short generally with decrease of the tail water depth, as the value of U shown in Eq. (115) in the case is equal to U_w expressed by Eq. (116). It seems, therefore, that the tendency described above corresponds to the case of $h'/h_0>1$ in the formula of Iowa University.

(iii) Considerations for determining the length of an apron : Two practical examples for the design of the length of an apron downstream of an outlet under the criterion for scour are described on the basis of the empirical formulas and the design charts described already. Furthermore, some considerations on the design of the apron are briefly discussed.

a) Example (1) : Calculate the relation between the length of an apron and the tail water depth under the condition that $U=5$ m/s and $D=0.5$ m for the characters of an outlet and the grain size of sand gravels at or near the downstream end of the apron is equal to $d=6.0$ cm.

Now it is necessary, first of all, to examine whether the apron can or cannot be designed in the region of $L/D\leq 10.4$ under the given condition. Estimating the necessary length L from Fig. 35 by using $U=5$ m/s and $d=6.0$ cm, $L=80$ m is obtained, and $L/D=160>10.4$. Then the apron cannot be designed in the region. Therefore, the design in the region of $L/D>10.4$ should be considered as is described below.

Since the tail water depth, where the hydraulic jump may occur just at the outlet under the given condition of the opening of the outlet and the velocity, is $h_0=1.35$ m from the theoretical relationship expressed by

$$h_0/D=(1/2)(\sqrt{1+8F_{rD}^2}-1),\quad F_{rD}^2=\alpha_1 U^2/gD.$$

In the above equations, α_1 is the coefficient of velocity profiles and is equal to unity in the above calculation. The outlet to be considered is in the case of $h_0>1.35$ m. Calculating the relation between $(U^2D)_w$ and L corresponding to the case of $d=6.0$ cm from Fig. 36 as described in c) of 2), (i), the final result becomes as is shown in Fig. 37 by the thick solid line. The relation between $(U^2D)_w$ and L in the case of $d=6.0$ cm is also shown in the figure by the fine solid line. Denoting the intersections of the thick and fine lines by B, C, D, E and F corresponding to $h_0=1.35$,

2, 3, 4 and 6 m respectively, the point of D, for example, designates the location for determining the necessary length of the apron, and from this the necessary length can be obtained as $L=14.9$ m. That is to say, the fact is presented that the apron having a length of 14.9 m is sufficient to protect against scour if the tail water depth is less than 3 m, but on the contrary if the tail water depth becomes greater than 3 m, the apron is dangerous for scour. The intersection of the straight line of $(U^2D)_w=U^2D$ shown in the figure by the broken line and the thick solid line, denoted by G, shows the case where $h_0/L=0.288$, and this means that the theoretical necessary length of an apron for protection against scour does not change for the greater depth than $h_0=9.16$ m. The range is of $10.4\leq L/D<\xi_e$, which is the zone of established flow, and the location of G in the figure should change necessarily with the value of U^2D. The point of A, which shows the location of $L/D=10.4$, is unimportant in the present case, as the range where $h_0<1.35$ m occurs the super-critical flow, and the apron fitting to prevent the bed from scour cannot be constructed in the region of $L/D<$ 10.4 already described.

Moreover, the points of b, c, d, e, and f satisfy $h_0/L=0.288$ for the values of $(U^2D)_w=U^2D$ corresponding to the points respectively, and describe the same significance as the point of G. For the determination of the necessary length of an apron in the case where the super-critical flow appears in downstream of an outlet, the method described here cannot be applied, though the results obtained in the preceding paper by the author[9] will practically be available to estimate the length of an apron.

b) Example (2): Now consider the outlet, as shown in Fig. 13, under the conditions that the water depth, denoted by H, upstream of the outlet is constant, the control section for water profiles is in the downstream end far from the outlet, and the flow downstream of the outlet is assumed to be approximately uniform flow. For the above outlet, $H=5.0$ m, the discharge coefficient of the outlet $C_q=0.4$, the characters of the connecting channel downstream of the outlet, that is, the channel slope $i_0=1/3600$ and the Manning coefficient $n=0.02$ s/m$^{1/3}$, and the size of sand gravels downstream of the apron $d=4.0$ cm, are given. Consider the change of the necessary length for the criterion for scour in the case when the opening of the outlet is operating very slowly.

Under the above assumptions, the discharge from the outlet q can be

written as

$$q(=UD)=C_q\sqrt{2g(H-h_0)}D$$

and the Manning formula can be expressed as

$$q(=UD)=\frac{1}{n}h_0^{5/3}i_0^{1/2}$$

for the relation among the discharge, the tail water depth, the slope of the bed and the Manning coefficient. Then, if the values of C_q, n and i_0 are given, the values of U and h_0 can be calculated as the functions of D only.

Calculating the necessary length of an apron from the values of U, h_0 and d computed above, by the same method as used in Fig. 37, the results shown in Fig. 38 can be obtained. On the other hand, whether the flow downstream of an outlet is super-critical or not could be considered in the same way as in the example (1). It is found from the consideration that the super-critical flow does not appear for all of the values of D in practice. The value of L should be calculated from Fig. 35 for the range of L/D lesser than 10.4, so the relation between the necessary length of an apron and the opening of the outlet is presented in the figure by the thick solid line beginning discontinuously from the point B as limited to the point A.

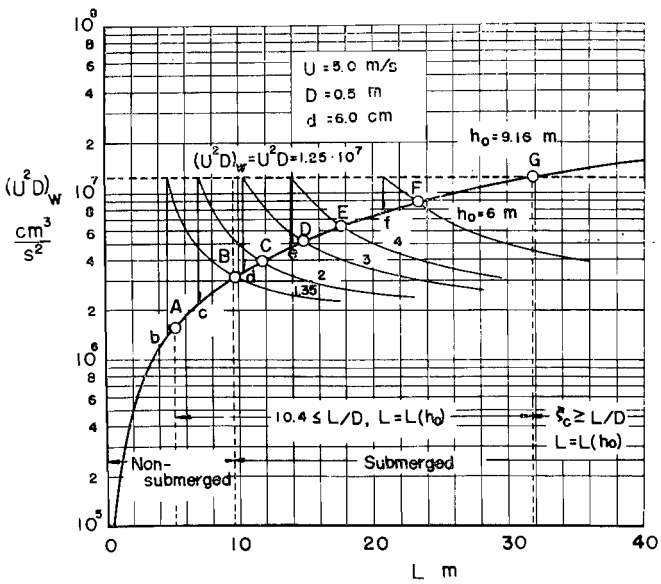

Fig. 37. Numerical example for design of length of apron (1); relation between quantity of $(U^2D)_w$ and length of apron.

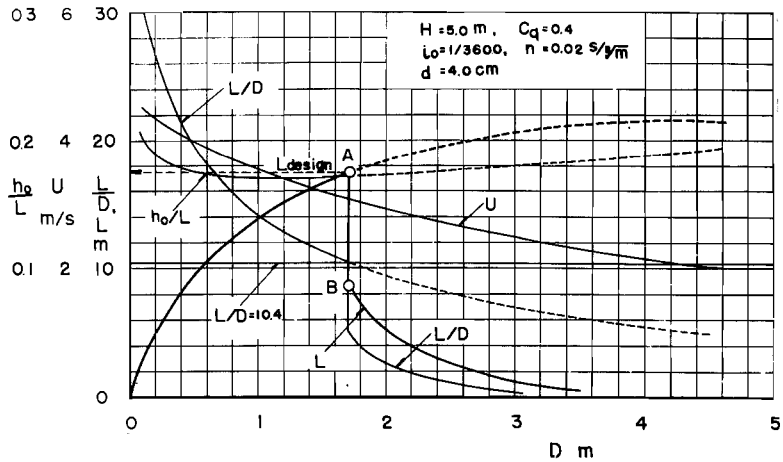

Fig. 38. Numerical example for design of length of apron (2); variations in velocity of outlet, tail water depth and necessary length of an apron with opening of outlet.

Since $h_0/L<0.288$ except for the case where the value of D is very small, it is clear that the range of D lesser than $D=1.71$ m given by the point A is $L/D>\xi_e$, and on the contrary, the range of $D>1.71$ m is $L/D<10.4$. It is disclosed from the results that the theoretical length of an apron in the case when the opening of the outlet is operating very gradually, increases rapidly in the range of the small value of D, and becomes maximum at the point A in which $L/D=10.4$, and furthermore, decreases rapidly with the increase of the opening. Hence the value of L shown in the figure by L_{design} which is equal to 17.5 m, should be recommended for the necessary length of the apron in the design.

In the practical examples described above, the necessary length of an apron for the criterion for scour is estimated under the given conditions for the sand gravels downstream of the apron. On the contrary, however, it can easily be considered to the necessary size of the sand gravels downstream of an apron for preventing the bed from scour at or near the downstream end of the apron.

Based on the above practical examples and the empirical formulas for determining the necessary length of an apron, some considerations on the design of the apron are briefly discussed and the author's view for the design is also described below.

In the case where the length of an apron is in the region of $L/D\leq 10.4$,

the length is proportional to $U^9 d^{-n'}$ in which n' is from 5/3 to 5, so that the velocity of the outlet should be small for the economical design of the apron. And use of the large-size sand gravels will be effective for the purpose. As is seen from the above examples, however, the apron has not been constructed in the region of flow establishment in general, and the case will be used only for an outlet or a culvert having low head of fall. For the apron which will be constructed in the range of $10.4 \leq L/D < \xi_c$, the length is proportional to $(U^2D)^{7/8}\ d^{-n'}$ in which n' is from 5/8 to 15/16, so that the decrease of U is more effective than the decrease of D to shorten the necessary length. The velocity should be given as small as possible for design discharge. In addition, it is clear that the use of large-size sand gravels is very effective to shorten the length of an apron, since the length in the range is nearly inversely proportional to the size. By the decrease in the tail water depth within the range of $h_0/L > 0.288$, as is seen from Fig. 37, the necessary length of an apron can be shortened, but the estimation of the tail water depth should generally be used with circumspection as the depth will vary with the hydraulic condition at the end of a stream channel. It will be concluded from the above fact that the control of the tail water depth may be one of the effective methods to prevent the bed from scour downstream of the apron being already constructed. For practical purposes, an adequate estimation of the necessary tail water depth should be taken by the same graphical expression as Fig. 37. Taking the above conclusions into considerations, it will be infered that it is generally desirable to design the apron in the region of $h_0/L > 0.288$ for the case where the tail water depth is always constant.

For the apron as described in the second example, the maximum value of the necessary length of an apron exists theoretically in operating the outlet. The estimation will firmly be made by the procedure described already. Although the discharge coefficient of an outlet has been assumed to be constant in the example for simplifying the numerical computation, the change of the coefficient with the tail water depth should be taken into the consideration for a more exact estimation of the necessary length of an apron[14]

In the considerations described above, the apron has been assumed to be of a smooth bed, but the existing apron is never smooth. It can be supposed from the results obtained in the second chapter and the theoreti-

cal and experimental considerations on the criterion for scour, that the estimation in the above examples may generally be safely used. On the other hand, in order to make the length of an apron as short as possible by decreasing tractive force of flow, the apron with suitable rough beds will be used in practical problems. Since, however, the function of drainage of a culvert or an outlet will decrease, the considerations on the problems should depend upon future studies.

4. Conclusion

In the introduction of this paper, some problems in design of the length of an apron to prevent local scour were briefly discussed, based on the results obtained by many authorities. In the second chapter, the boundary layer growth in wall jets issuing from a submerged outlet in connection with the criterion for scour from wall jets was analyzed and considered on the basis of the momentum equation of a boundary layer, and compared with the experimental results. From the theoretical and experimental considerations, the followings may be summerized and concluded: 1) The main flows are relatively in good agreement with the results of two-dimensional turbulent jets, and the limit of applicability has been disclosed. 2) The velocity profiles in the boundary layer and the resistance law are closely connected with the diffusion of jets, and the local skin friction coefficient in the zone of established flow is much greater than the Blasius law. 3) The results of computation for the boundary layer growth using the resistance law based on the experimental results, are in fairly good agreement with the experimental results, and the limit of applicability has been presented. 4) The theoretical curves of the shear velocity along the bed are also in good agreement with experimental data, and the shear velocity decreases rapidly with the distance from an outlet.

In the third chapter, the criterion for scour from wall jets issuing from a submerged outlet was considered theoretically by fully applying the results of the boundary layer growth in wall jets obtained in the second chapter. From the theoretical considerations, it was disclosed that the criterion for scour from wall jets in both regions of flow establishment and established flow are presented by the three parameters, $u_c^{*2}/(\sigma/\rho-1)gd\tan\varphi$, u_c^*d/ν and u_c^*/U or u_c^*/u_0. It was clarified by comparing the above theoretical

results with the critical tractive force and the criterion for scour from flows downstream end of a smooth bed in uniform flow that a parameter u_c*/U or u_c*/u_0 should be added, the effects of which on the criterion are very complicated and may be not large, especially in the region of established flow. And it was concluded from the comparison between the theoretical curves and that for the critical tractive force that the criterion for scour from wall jets is presented by the lesser critical shear velocity than that for the critical tractive force in the region of sufficiently large u_c*d/ν.

The theoretical results on the criterion for scour for both regions of flow establishment and established flow was compared with the experimental results, and it was disclosed that the theoretical curves for the criterion were in fairly good agreement with the experimental results, although the theoretical considerations included many assumptions in the development.

The criterion for scour in the region where the results on wall jets cannot be applied owing to the existence of a free water surface was considered by means of the dimensional analysis based on the theoretical results for the former two regions. It was made clear that the most important parameter in the criterion for scour was the ratio of the tail water depth to the length of an apron and the relation was disclosed and decided by the experimental results.

Moreover, the empirical formulas for the criterion for scour from wall jets and for determining the necessary length of an apron for complete protection against scour were proposed and discussed on the basis of the theoretical and experimental considerations. Design charts available to practical problems in design of an apron were developed.

The author believes that the foregoing results can serve as the fundamental data for design of the apron of a culvert and an outlet, to prevent scour. Furthermore, the results obtained in this paper will be applicable to analyze hydraulically the mechanism of scour downstream of an apron, so the application will be presented in a later paper.

Acknowledgments

The author is greatly indebted to Professors Tojiro Ishihara and Yuichi Iwagaki, Kyoto University, for their constant instruction during this study, and also thanks are due to Messrs. M. Kuge, T. Uno, N. Tsuji and J.

Hasegawa for their assistance in the experiments and computations.

A part of this investigation was supported by the Science Research Expences of the Ministry of Education and thanks are due to the Ministry of Education.

References

1) Leliavsky, S. : Irrigation and Hydraulic Design, Vol. 1, Chapman & Hall, London, 1955, p. 204.
2) Bligh, W. G. : Dams and Weirs, American Technical Society, Chicago, 1918, p. 164.
3) Leliavsky, S. : Irrigation and Hydraulic Design, Vol. 1, Chapman & Hall, London, 1955, p. 208.
4) Veronese, A. Erosioni di fondo avalle di uno scarcio, Annali dei Lavori Publici, 1937, p. 717.
5) Ahmad, N. : Mechanism of Erosion below Hydraulic Works, Proc. Minnesota Int. Hyd. Conv., I.A.H.R., 1953, pp. 133–143.
6) Minami, I. Hydraulic Studies of Dams and Weirs, Thesis for Degree, 1960, p. 4, (in Japanese).
7) Iwagaki, Y. : Hydrodynamical Study on Critical Tractive Force, Trans. J.S.C.E., No. 41, 1956, pp. 1–21, (in Japanese).
8) Iwagaki, Y. and Tsuchiya, Y. : On the Critical Tractive Force for Gravels on a Granular Bed in Turbulent Streams. Trans. J.S.C.E., No. 41, 1956, pp. 22–38, (in Japanese).
9) Tsuchiya, Y. Criterion for Scour at the Downstream End of a Smooth Bed, Trans. J.S.C.E., No. 80, 1962, pp. 18–30, (in Japanese).
10) Halbronn, G. Etude de la mise en régime des écoulements sur les ouvrages à forte pente, La Houile Blanche, No. 1, 1952, pp. 21–40.
11) Graya, A. E. and Delleur, J. W.: An Analysis of Boundary Layer Growth in Open Conduits near Critical Regime, Dept. of Civil Eng., Columbia Univ., CU–1–52–ONR–226, 1952.
12) Bauer, J. W. : Turbulent Boundary Layer on Steep Slopes, Proc. A.S.C.E., Sep. No. 281, 1953.
13) Iwasa, Y. Boundary Layer Growth of Open Channel Flows on a Smooth Bed and Its Contribution to Practical Application to Channel Design, Memoirs of Fac. of Eng., Kyoto Univ., Vol. 19, No. 3, 1957, pp. 229–254.
14) Henry, H. R. . Discussion of "Diffusion of Submerged Jets", Trans. A.S.C.E., Vol. 115, 1950, pp. 665–697.
15) Tsubaki, T. and Furuya, A. . A Consideration on the Submerged Flow, Report of the Institute of Appl. Mech., Kyushu Univ., No. 3, 1952, pp. 61–64, (in Japanese).
16) Albertson, M. L., Dai, Y. B., Jensen, R. A., and Rouse, H. Diffusion of Submerged Jets, Trans. A.S.C.E., Vol. 115, 1950, pp. 639–697.
17) Glauert, M. B. The Wall Jet, Jour. of Fluid Mech., Vol. 1, 1956, pp. 625–643.
18) Bakke, P. : An Experimental Investigation of a Wall Jet, Jour. of Fluid Mech.,

Vol. 2, 1956, pp. 467–472.
19) Schwarz, W. H. and Cosart, W. P. : The Two-Dimensional Turbulent Wall-Jet, Jour. of Fluid Mech., Vol. 11, 1961, pp. 481–495.
20) Iwagaki, Y. and Tsuchiya, Y. : Boundary Layer Growth in Wall Jets Issuing from a Submerged Outlet, Proc. 9th Japan National Cong. for Appl. Mech., 1959, pp. 259–264.
21) Tollmien, W. : Berechnung turbulenter Ausbreitungsvorgänge, Z.A.M.M., Vol. 6, 1926, S. 468–478.
22) Kuethe, A. M. Investigations of the Turbulence Mixing Regions Formed by Jets, Jour. of Appl. Mech., Vol. 2. No. 3, 1935, pp. A–87–95.
23) Schlichting, H. : Boundary Layer Theory, McGraw-Hill, 1955, p. 498.
24) Spengos, A. C. Turbulent Diffusion of Momentum and Heat from a Smooth, Plane Boundary with Zero Pressure Gradient, Scientific Report No. 1, Colorado Agri. and Mech. College, Colorado, 1956, pp. 1–50.
25) Taylor, G. I. Statistical Theory of Turbulence, Part IV Diffusion in a Turbulent Air Stream, Proc. Roy. Soc., A 151, 1935, pp. 465–478.

Publications of the Disaster Prevention Research Institute

The Disaster Prevention Research Institute publishes reports of the research results in the form of bulletins. Publications not out of print may be obtained free of charge upon request to the Director, Disaster Prevention Research Institute, Kyoto University, Kyoto, Japan.

Bulletins :

No. 1 On the Propagation of Flood Waves by Shoitiro Hayami, 1951.

No. 2 On the Effect of Sand Storm in Controlling the Mouth of the Kiku River by Tojiro Ishihara and Yuichi Iwagaki, 1952.

No. 3 Observation of Tidal Strain of the Earth (Part I) by Kenzo Sassa, Izuo Ozawa and Soji Yoshikawa. And Observation of Tidal Strain of the Earth by the Extensometer (Part II) by Izuo Ozawa, 1952.

No. 4 Earthquake Damages and Elastic Properties of the Ground by Ryo Tanabashi and Hatsuo Ishizaki, 1953.

No. 5 Some Studies on Beach Erosions by Shoitiro Hayami, Tojiro Ishihara and Yuichi Iwagaki, 1953.

No. 6 Study on Some Phenomena Foretelling the Occurrence of Destructive Earthquakes by Eiichi Nishimura, 1953.

No. 7 Vibration Problems of Skyscraper. Destructive Element of Seismic Waves for Structures by Ryo Tanabashi, Takuzi Kobori and Kiyoshi Kaneta, 1954.

No. 8 Studies on the Failure and the Settlement of Foundations by Sakurō Murayama, 1954.

No. 9 Experimental Studies on Meteorological Tsunamis Traveling up the Rivers and Canals in Osaka City by Shoitiro Hayami, Katsumasa Yano, Shohei Adachi and Hideaki Kunishi, 1955.

No.10 Fundamental Studies on the Runoff Analysis by Characteristics by Yuichi Iwagaki, 1955.

No.11 Fundamental Considerations on the Earthquake Resistant Properties of the Earth Dam by Motohiro Hatanaka, 1955.

No.12 The Effect of the Moisture Content on the Strength of an Alluvial Clay by Sakurō Murayama, Kōichi Akai and Tōru Shibata, 1955.

No.13 On Phenomena Forerunning Earthquakes by Kenzo Sassa and Eiichi Nishimura, 1956.

No.14 A Theoretical Study on Differential Settlements of Structures by Yoshitsura Yokoo and Kunio Yamagata, 1956.

No.15 Study on Elastic Strain of the Ground in Earth Tides by Izuo Ozawa, 1957.

No.16 Consideration on the Mechanism of Structural Cracking of Reinforced Concrete Buildings Due to Concrete Shrinkage by Yoshitsura Yokoo and S. Tsunoda. 1957.

No.17 On the Stress Analysis and the Stability Computation of Earth Embankments by Kōichi Akai, 1957.

No.18 On the Numerical Solutions of Harmonic, Biharmonic and Similar Equations by the Difference Method Not through Successive Approximations by Hatsuo Ishizaki, 1957.

No.19 On the Application of the Unit Hydrograph Method to Runoff Analysis for Rivers in Japan by Tojiro Ishihara and Akiharu Kanamaru, 1958.

No.20 Analysis of Statically Indeterminate Structures in the Ultimate State by Ryo Tanabashi, 1958.

No.21 The Propagation of Waves near Explosion and Fracture of Rock (I) by Soji Yoshikawa, 1958.

No.22 On the Second Volcanic Micro-Tremor at the Volcano Aso by Michiyasu Shima, 1958.

No.23 On the Observation of the Crustal Deformation and Meteorological Effect on It at Ide Observatory and On the Crustal Deformation Due to Full Water and Accumulating Sand in the Sabo-Dam by Michio Takada, 1958.

No.24 On the Character of Seepage Water and Their Effect on the Stability of Earth Embankments by Kōichi Akai, 1958.

No.25 On the Thermoelasticity in the Semi-infinite Elastic Soid by Michiyasu Shima, 1958.

No 26 On the Rheological Characters of Clay (Part 1) by Sakurō Murayama and Tōru Shibata, 1958.

No.27 On the Observing Instruments and Tele-metrical Devices of Extensometers and Tiltmeters at Ide Observatory and On the Crustal Strain Accompanied by a Great Earthquake by Michio Takada, 1959.

No.28 On the Sensitivity of Clay by Shinichi Yamaguchi, 1959.

No.29 An Analysis of the Stable Cross Section of a Stream Channel by Yuichi Iwagaki and Yoshito Tsuchiya, 1959.

No.30 Variations of Wind Pressure against Structures in the Event of Typhoons by Hatsuo Ishizaki, 1959.

No.31 On the Possibility of the Metallic Transition of MgO Crystal at the Boundary of the Earth's Core by Tatsuhiko Wada, 1960.

No.32 Variation of the Elastic Wave Velocities of Rocks in the Process of Deformation and Fracture under High Pressure by Shogo Matsushima, 1960.

No.33 Basic Studies on Hydraulic Performances of Overflow Spillways and Diversion Weirs by Tojiro Ishihara, Yoshiaki Iwasa and Kazune Ihda, 1960.

No.34 Volcanic Micro-tremors at the Volcano Aso by Michiyasu Shima, 1960.

No.35 On the Safety of Structures Against Earthquakes by Ryo Tanabashi, 1960.

No.36 On the Flow and Fracture of Igneous Rocks and On the Deformation and Fracture of Granite under High Confining Pressure by Shogo Matsushima, 1960.

No.37 On the physical properties within the B-layer deduced from olivine-model and on the possibility of polymorphic transition from olivine to spinel at the 20° Discontinuity by Tatsuhiko Wada, 1960.

No.38 On Origins of the Region C and the Core of the Earth ——Ionic-Intermetallic-Metallic Transition Hypothesis—— by Tatsuhiko Wada, 1960.

No.39 Crustal Stucture in Wakayama District as Deduced from Local and Near Earthquake Observations by Takeshi Mikumo, 1960.

No.40 Earthquake Resistance of Traditional Japanese Wooden Structures by Ryo Tanabashi, 1960.

No.41 Analysis With an Application to Aseismic Design of Bridge Piers by Hisao Goto and Kiyoshi Kaneta, 1960.

No.42 Tilting Motion of the Ground as Related to the Volcanic Activity of Mt. Aso and Micro-Process of the Tilting Motion of Ground and Structure by Yoshiro Itō, 1961.

No.43 On the Strength Distribution of the Earth's Crust and the Upper Mantle, and

the Distribution of the Great Earthquakes with Depth by Shogo Matsushima, 1961

No.44 Observational Study on Microseisms (Part 1) by Kennosuke Okano, 1961.

No.45 On the Diffraction of Elastic Plane Pulses by the Crack of a Half Plane by Michiyasu Shima, 1961.

No.46 On the Observations of the Earth Tide by Means of Extensometers in Horizontal Components by Izuo Ozawa, 1961.

No.47 Observational Study on Microseisms (Part 2) by Kennosuke Okano, 1961.

No.48 On the Crustal Movement Accompanying with the Recent Activity on the Volcano Sakurajima (Part 1) by Keizo Yoshikawa, 1961.

No.49 The Ground Motion Near Explosion by Soji Yoshikawa, 1961.

No.50 On the Crustal Movement Accompanying with the Recent Activity of the Volcano Sakurajima (Part 2) by Keizo Yoshikawa, 1961.

No.51 Study on Geomagnetic Variation of Telluric Origin Part 1 by Junichiro Miyakoshi, 1962.

No.52 Considerations on the Vibrational Behaviors of Earth Dams by Hatsuo Ishizaki and Naotaka Hatakeyama, 1962.

No.53 Some Problems on Time Change of Gravity (Parts 1 and 2) by Ichiro Nakagawa, 1962.

No.54 Nature of the Volcanic Micro-Tremors at the Volcano Aso, Part 1. Observation of a New Type of Long-Period Micro-Tremors by Long-Period Seismograph by Kosuke Kamo, 1962.

No.55 Nature of the Volcanic Micro-Tremors at the Volcano Aso, Part 2. Some Natures of the Volcanic Micro-Tremors of the 1st kind at the Volcano Aso by Kosuke Kamo, 1962.

No.56 Nonlinear Torsional Vibration of Structures due to an Earthquake by Ryo Tanabashi, Takuji Kobori and Kiyoshi Kaneta, 1962.

No.57 Some Problems on Time Change of Gravity (Parts 3, 4 and 5) by Ichiro Nakagawa, 1962.

No.58 A Rotational Strain Seismometer by Hikaru Watanabe, 1962.

No.59 Hydraulic Model Experiment Involving Tidal Motion (Parts 1, 2, 3 and 4) by Haruo Higuchi, 1963.

No.60 The Effect of Surface Temperature on the Crustal Deformations by Shokichi Nakano, 1963.

No.61 An Experimental Study on the Generation and Growth of Wind Waves by Hideaki Kunishi, 1963.

No.62. The Crustal Deformations due to the Source of Crack Type (1) by Shokichi Nakano, 1963.

No.63. Basic Studies on the Criterion for Scour Resulting from Flows Downstream of an Outlet by Yoshito Tsuchiya, 1963.

Bulletin No. 63 Published June, 1963

昭和 38 年 6 月 10 日 印 刷
昭和 38 年 6 月 15 日 発 行
編輯兼
発行者 京都大学防災研究所
印刷者 山 代 多 三 郎
京都市上京区寺之内通小川西入
印刷所 山代印刷株式会社